MANIPULATION OF THE GUT MICROBIOTA ATTENUATES THE NEGATIVE EFFECTS OF HIGH-FAT DIET

by

ELIZABETH A. KLINGBEIL

(Under the Direction of Claire de La Serre)

ABSTRACT

Consumption of a high-fat (HF) diet has been shown to increase risk of metabolic disorders such as obesity and diabetes. These comorbidities are a major health problem in westernized countries, including the United States, where HF diets are increasingly popular. Obesity has been long-defined as a chronic, low-grade, systemic inflammatory state and the integrity of the gastrointestinal (GI) tract has been found to contribute to this. Increased GI permeability due to changes in gut microbiota composition in response to HF diet allows for the translocation of pro-inflammatory bacterial byproducts, such as lipopolysaccharide (LPS). Currently, there is little research investigating potential diet interventions to maintain gut microbiota composition, preserve gut integrity and gut-brain satiety signaling. Therefore, the objective of this dissertation is to investigate the effects of diet interventions in prevention of the negative metabolic outcomes related to HF diet. I hypothesized that promoting a gut microbiota composition in rodents closer to a control low fat (LF) diet would attenuate the effects of HF diet. For both studies, male Wistar rats were fed a 45% HF diet for 7-8 weeks and either supplemented with a prebiotic (potato resistant starch, Chapter 2) or pair-fed to modulate timing of feeding (Chapter 3). For both studies, weight and food intake, microbiota composition,

inflammatory status, glucose homeostasis, satiety response and vagal signaling were assessed. In the potato study (Chapter 2), resistant starch (RS) supplementation prevented microbiota dysbiosis and HF diet-induced inflammation. Functionally, RS prevented hyperphagia, loss in glucose homeostasis, satiety sensitivity and hindbrain unmyelinated c fibers associated with HF diet. In the second study (Chapter 3), timing of feeding, regardless of diet composition, was shown to favorably manipulate microbiota composition. Rats pair-fed HF diet just before the onset of their active (dark) cycle ate the same calories but consumed significantly fewer meals. Pair-feeding improved microbiota dysbiosis, inflammation status and glucose tolerance associated with HF diet. The studies of this dissertation suggest that microbiota manipulation via prebiotic supplementation or feeding pattern modulation preserve gut microbiota composition, preventing low-grade systemic inflammation associated with loss in glucose homeostasis and satiety signaling, avoiding the onset of obesity and other metabolic disorders.

INDEX WORDS: gut microbiota, inflammation, glucose homeostasis, vagal signaling, satiety, potato resistant starch, time-restricted feeding

MANIPULATION OF THE GUT MICROBIOTA ATTENTUATES THE NEGATIVE EFFECTS OF HIGH-FAT DIET

by

ELIZABETH A. KLINGBEIL

B.A., Concordia College, 2016

A Dissertation Submitted to the Graduate Faculty of The University of Georgia in Partial Fulfillment of the Requirements for the Degree

DOCTOR OF PHILOSOPHY

ATHENS, GEORGIA

2020

MANIPULATION OF THE GUT MICROBIOTA ATTENTUATES THE NEGATIVE EFFECTS OF HIGH-FAT DIET

by

ELIZABETH A. KLINGBEIL

Major Professor:	Claire de La Serre
Committee:	Jamie Cooper
	Philip Holmes
	Emma Laing
	Emily Noble

Electronic Version Approved:

Ron Walcott
Interim Dean of the Graduate School
The University of Georgia
August 2020

DEDICATION

This dissertation is dedicated to my parents—Paul and Cindy Klingbeil—without your love, grace and unending patience, I would not have been able to accomplish this; to my siblings—Jocelyn and Jordan Rodgers and Ben Klingbeil—without your wisdom and humor, I would not have found the confidence to complete my program; and to my dear friend—Hannah Wilson—without your support and understanding, I would not have survived the difficult moments.

ACKNOWLEDGEMENTS

Thank you to everyone in the Gastrointestinal Neurophysiology Lab for your help and effort over the last four years. Without your insights, this dissertation would not have been accomplished. To Claire, thank you for your guidance and the time you gave me. You saw potential in myself I did not, allowed me to excel in areas that I enjoyed and pushed me to accomplish things I never would have on my own. To Dr. Barbara Grossman, thank you for giving me every opportunity to excel as a nutrition professional. I will hold my time under your direction as a dietetic intern close to my heart. I would also like to acknowledge faculty in the Foods and Nutrition department that have given me wisdom, teaching, training and so many other life skills. Our department is a wealth of knowledge, and I am very grateful to have spent a significant amount of time gleaning from it.

TABLE OF CONTENTS

Page

LIST OF TABLES

Page

LIST OF FIGURES

Page

CHAPTER 1

INTRODUCTION AND LITERATURE REVIEW[1]

Introduction

Obesity and associated comorbidities have increased dramatically in the United States [1]. Obesity is a chronic, systemic, inflammatory state [2] and recent data have suggested that loss of gut barrier integrity may contribute to this inflammatory state [3]. Although there is accumulating evidence that gut microbiota composition influences gut integrity and systemic inflammatory status [4-6], little research has focused on the protective effects of specific diet interventions (resistant starch, feeding patterns) on glucose homeostasis and gut-brain satiation signaling. My dissertation studies will address gaps in the literature investigating the effect of diet interventions on microbiota composition and how they maintain glucose homeostasis and gut-brain satiation signaling lost with a high-fat diet. This research will contribute to the development of potential dietary treatments addressing the ongoing obesity health crisis.

The gastrointestinal (GI) microbiome is composed of more than 10^{14} bacteria encompassing over 400 different species [7]. These bacteria inhabit the entirety of our GI tract. In recent years, gut microbiota have been shown to play a crucial role in host physiology and pathophysiology, including regulation of energy homeostasis and obesity [8, 9]. Two phyla, *Firmicutes* and *Bacteriodetes,* comprise 80-90% of the bacteria in the GI tract. Other, less represented phyla in the gut are *Proteobacteria*, *Actinobacteria*, *Fusobacteria*, and

[1] Adapted from Klingbeil EA and de La Serre CB. Microbiota modulation by eating patterns and diet composition: impact on food intake. Am J Physiol Regul Integr Comp Physiol 2018;315(6):R1254-R1260. Reprinted here with permission of publisher.

Verrucomicrobacteria [7]. Microbiota composition is heavily influenced by the environment, especially by the diet [10]. The effects of dietary fats consumption on microbiota composition has been determined in different models. The "high fat diet (HFD)/obese-type" microbiota is characterized by an increased *Firmicutes* to *Bacteriodetes* ratio, a decreased bacterial diversity and an increased pro-inflammatory potential [8, 9]. This pro-inflammatory potential is associated with increased gut permeability and elevated circulating levels of lipopolysaccharide (LPS), a condition known as metabolic endotoxemia [11]. Metabolic endotoxemia is a state of chronic low-grade inflammation and is sufficient to promote food intake and weight gain [12]. Microbiota-originating inflammation notably alters vagal input to the brain, particularly vagally-mediated response to satiation cues [12]. The vagus nerve relays information regarding quantity and quality of nutrients present in the GI tract to the nucleus of solitary tract (NTS) in the brainstem to regulate meal size [12]. HFD consumption leads to remodeling of the vagal afferent pathway; however these changes, along with weight gain, are absent in HFD-fed male rats when microbiota composition is normalized [13]. Taken together, these data support a role for microbiota dysbiosis in the development of obesity. The purpose of this review is to outline how modulation of the microbiota by dietary macronutrient composition and eating patterns can influence host eating behavior.

Dietary modulation of the gut microbiota

Fat content: Diet composition is a major regulator of gut microbiota composition [10]. The modern-day Western diet consists of readily available, energy-dense foods rich in sugars and fats. Chronic intake of energy-dense food has been linked to obesity [14]. Obesity in humans and animal models is characterized by abnormal gut microbiota composition, or dysbiosis [8]. In rodent models, dysbiosis can be induced by consumption of a western-type diet. Feeding animals

a HFD notably promotes a microbiota profile similar to that of obese male subjects [3, 6, 15]. In male rodents, HFD-driven changes in microbiota composition include an increase in *Firmicutes:Bacteriodetes* ratio driven by increases in *Erysipelotrichales* and *Clostridiales* abundances, two orders belonging to the phylum *Firmicutes*. Similarly, in humans, adiposity is associated with an increase in the *Firmicutes:Bacteriodetes* ratio [8]. In male animal models, HFD is also associated with decreases in *Prevotellaceae* and *Rikenellaceae* (families in the *Bacteriodetes* phylum) abundances as well as abundances in several genera of the *Clostridiaceae* family (*Firmicutes*) [6, 13]. HFD consumption has also been reported to increase *Proteobacteria* abundance while decreasing abundance of probiotics such as *Bifidobacteria* [16]. *Proteobacteria* are gram-negative, LPS carrying, pro-inflammatory bacteria [17]. Bacterial products such as LPS can activate pattern recognition receptors, like Toll-like receptors (TLR), on the apical and basolateral side of intestinal epithelial cells (IEC) leading to cytokine release [18]. The proteobacteria *Sutterella*, for example, can trigger IL-8 production from enterocytes [19]. Pro-inflammatory cytokines promote cytoskeleton protein phosphorylation and contraction, impairing the epithelial barrier integrity [3, 20]. A damaged epithelial barrier can allow the translocation of bacterial products, including LPS, into the circulation. In human males [21] and male rodents [3] consumption of energy dense foods is associated with an increase in circulating pro-inflammatory bacterial factors like LPS. Pro-inflammatory effects of HFD on microbiota composition may be mediated by a diet-driven increase in release of bile acids, as bile acids have been found to alter the cecal microbiota composition in male rats [22]. Bile acids have the capacity to impact microbiota composition by promoting bile acid-metabolizing bacteria and preventing the growth of bacteria sensitive to bile acids [23].

Gut microbiota composition is sufficient to induce adiposity independently of diet. In microbiota-depleted male animals, the obese phenotype can be transferred via colonization with dysbiotic microbiota from obese animals [15]. Moreover, in animal models that are sensitive to diet-induced obesity (DIO), microbiota dysbiosis is necessary to trigger weight gain. In Sprague-Dawley male rats, HFD-driven microbiota dysbiosis precedes the development of obesity, and normalization of the microbiota composition hinders diet-driven weight gain [13]. Similarly, probiotics or antibiotics usage prevents weight gain in response to HFD-feeding in male C57 mice [24, 25]. Taken together, these data support a causal role for diet-driven dysbiosis in the development of obesity. However, it should be noted that there is evidence of obese mice displaying a "normal" microbiota [26] and that some dysbiotic male rats are resistant to DIO [3]. Interestingly, these DIO resistant animals maintain an intact intestinal epithelial barrier, normal circulating LPS and inflammatory marker levels, and do not develop hyperphagia when fed with a HFD [3]. Similarly to diet, dysbiosis can be seen as a challenge for the organism with variability in individual responses. Together these findings suggest that the development of dysbiosis-associated inflammation may be critical the etiology of obesity and associated metabolic abnormalities.

Sugar content: Refined HFD can also be rich in sugars, and there is accumulating evidence showing that high amounts of dietary sugar (fructose or sucrose) can rapidly alter the gut microbiota. In male rats, consumption of a diet containing 17% fructose leads to a significant decrease in microbial diversity within a week of diet onset [6]. High sugar diet (HSD) induces changes in microbiota composition that are comparable to that with a HFD: an increase in *Firmicutes:Bacteriodetes* ratio and a significant decrease in *Bacilli* abundance, a well-established probiotic [6]. Male rats fed a HSD display an increase in liver fat deposition associated with

increases in the abundance of *Clostridia*, particularly the families *Ruminococcaceae* and *Lachnospiraceae*, which had previously been linked to fat accumulation [6]. A study by Magnusson *et al*. comparing a 42% HFD to a 62% HSD in male mice found a significant increase in *Clostridiales* and *Erysipelotrichales* abundances with consumption of HSD, along with a decrease in *Bacteroidales* abundance even greater than what was observed in the HFD group [27]. Additional studies looking at HSD consumption in male rats showed that—independently of body weight—sugar consumption affects the gut microbiome during juvenile and adolescent development by increasing *Betaproteobacteria* abundance (similarly to HFD consumption [16]) and decreasing *Prevotella* and *Lachnospiraceae* abundance [28].

Protein content: Research on protein and the gut microbiota has focused on transitioning obese animals from a HFD + HSD diet to a diet high in protein to investigate the potential anti-obesity effects of a high protein diet (HPD). Stengel *et al*. found that DIO rats that were switched from a HFD + HSD to a HPD reduced their daily food intake by 30% on day one and maintained a 14% reduction throughout the remaining two weeks of the study [29]. The same group of rats showed decreased body weight, maintained lean body mass, and had improved glucose control [29]. HPD consumption in male rats has been associated with an increase in *Bacteroides* and *Akkermansia spp.* abundances [30]. *Akkermansia spp*. belongs to a *Verrucomicrobia* phylum and has previously been found to have anti-obesity and anti-diabetic properties [31]. *Akkermansia* notably plays an important role in gut integrity by colonizing and feeding on gut mucus, while secreting acetate and propionate. The byproducts produced by *Akkermansia* stimulate immune function and metabolic signaling, providing a protective, anti-inflammatory effect [32] while propionate favors enterocyte differentiation and improve GI barrier function [33]. In contrast, HFD feeding leads to a decrease in *Akkermansia* abundance [34]. However, because weight loss

itself has been found to have similar effects on the gut microbiota [35], a HPD diet may have an indirect effect on gut microbiota via a reduction in body weight.

Fiber content: GI microbiota composition is a complex dynamic resulting from of what is present or absent in the diet in addition to the environmental conditions (pH, oxygen, etc). HFD and HSD used in research settings are generally prepared with refined ingredients and often lack soluble fibers when compared to regular laboratory chow [36]. Low levels of dietary fibers may be critical in HFD and HSD-driven dysbiosis. Dietary fibers play an important role in gut health, as they increase stool mass and decrease transit time, improving digestion and absorption. Additionally, fiber and other non-digestible carbohydrates, such as resistant starch, can be fermented by the commensal microbiota [37]. The major end products of this carbohydrate fermentation are short-chain fatty acids (SCFA), particularly acetate, propionate, and butyrate [38]. These weak acids lower the pH of the distal gut, preventing the growth of some gram-negative pathogenic bacteria who are sensitive to mildly acidic pH, including the proteobacteria *E.Coli* [39]. SCFA also act as trophic agents in the gut, promoting the differentiation of enterocytes and improving GI morphology, mucus secretion and overall intestinal epithelial barrier function [33]. Additionally, SCFA serve as endogenous ligands for free fatty acid receptors (FFAR) 2 and 3, two receptors that have been shown to control the secretion of gut satiation peptides, including glucagon-like peptide 1 (GLP-1) [40]. There is evidence that HFD-induced metabolic syndrome may be attributed to a lack of dietary fiber and bacterial fermentation. Inulin supplementation in HFD fed mice prevents DIO, and these effects are partially recapitulated via SCFA administration [36]. Other prebiotics, such as oligofructose, have also been found to ameliorate DIO [41], highlighting the key role for microbiota in modulating host physiology. Interestingly, in both male and female humans, significant changes

in gut microbiota composition were observed within 24 hours when a Western diet was replaced by a high fiber diet [42].

Eating patterns: IEC undergo cyclical gene expression that is affected by the host's circadian clock and feeding [43]. The GI microbiota is tightly linked to these IEC circadian regulators and as a result, experiences cyclic compositional changes which can be altered with the development of DIO [43]. In male rats fed a chow diet ad libitum, *Firmicutes* bloom during the fed state while *Bacteriodetes* and *Verrucomicrobia* abundances increase during the fasted state [43]. However, in DIO male rats fed a HFD ad libitum, *Firmicutes* remained dominant regardless of feeding state [43]. HFD fed male rats have been found to increase their intake during their inactive phase [44] and alteration in animal eating patterns directly influence microbiota composition. Complete alternate-day fasting, modified fasting regimens, and time-restricted feeding (TRF) have been found to "reprogram" oscillations of the gut microbiota [45]. Complete alternate-day fasting consists of days with no energy consumption alternating with days of ad libitum energy consumption. Modified fasting regimens involve consuming 20-25% of estimated energy needs on fasting days and consuming 100% of energy needs on intermittent days while TRF allows ad libitum energy intake for a specific time frame followed by periods of fasting. TRF on weekdays has been shown to reduce weight gain in HFD fed juvenile male rats (between 5 and 13 weeks of age) independently of caloric intake [44]. TRF is associated with increased production of SCFA, specifically acetate, propionate, and butyrate [46]. TRF also restores normal circadian cycling within the microbiota composition, characterized by an increase in *Firmicutes* abundance during the day and a decrease during the night [43]. Interestingly, TRF also promotes the growth of *Akkermansia muciniphila*, the SCFA-producing

bacteria previously mentioned [43].

Diet-induced dysbiosis and inflammation

The crucial role of the intestinal epithelial barrier: Diet-driven alteration in microbiota composition can promote an inflammatory state [3, 11]. Dysbiosis is associated with an increase in gram negative bacteria, which produce LPS [47]. Increased amounts of LPS in the gut result in TLR4 activation on IEC and release of pro-inflammatory cytokines [18, 48]. Tight junction (TJ) proteins control diffusion and leakage of digestive products between the GI tract and circulatory system. Cytokines released in the gut increase gut barrier permeability [48] by altering the TJ protein network, allowing for translocation of LPS and other bacterial products or metabolites across the epithelium [3]. Bacteria-driven inflammation is a key factor in altering host physiological functions. We have notably found in male rats that propensity for obesity is tightly associated with an increase in gut permeability and low grade inflammation while, DIO-resistant (DIO-R) animals maintain an intact intestinal epithelial barrier [3]. In human males, circulating levels of LPS are correlated with energy intake [49]. Similarly, in male rodents, chronic administration of low doses of LPS is sufficient to induce hyperphagia and weight gain [12] as well as insulin resistance [11]. Moreover, knocking out the LPS receptor in mice prevents DIO [50], supporting the hypothesis that bacteria-driven inflammation may have a causal role in the development of obesity.

Vagal inflammation and eating behavior: The vagus nerve plays a key role in controlling food intake, especially meal size. Enteroendocrine cells secrete gut peptides, including satiety peptides such as cholecystokinin (CCK), that can activate vagal afferents and relay information on the quantity and quality of nutrients present in the GI tract to the NTS in the brainstem [51]. Chronic HFD feeding has been shown to alter vagally-mediated satiety, resulting in larger meals

and an overall increase in energy intake [52]. Vagal afferent terminals reside in the lamina propria where they are ideally positioned to sense bacterial by-products. While there are other factors that change with diet-driven GI microbiota dysbiosis, the ability of LPS to induce hyperphagia corroborate the hypothesis that LPS plays a primary role in the bug-gut-brain axis. LPS has been found to activate vagal afferents [53] and can directly bind to TLR4 receptors located in the nodose ganglion (NG), where vagal afferent neuron cell bodies are located. LPS can also indirectly activate vagal afferents by promoting the release of cytokines such as IL-1β or TNF-from immune cells [53].

Chronic LPS administration in male and female rats leads to a significant increase in food intake [12, 54]. Similarly to other pro-inflammatory factors, LPS signaling also induces an anti-inflammatory feedback loop [55]. In particular, we have found that LPS treatment upregulates protein levels of suppressor of cytokine 3 (SOCS3) in the NG [12]. Interestingly, SOCS3 is known to inhibit signaling of the adiposity hormone leptin via phosphorylation of signal transducer and activator of transcription 3 (STAT3) [56]. A loss of vagal leptin sensitivity has been shown to impair CCK signaling [57]. In accordance with these data, LPS-infused male animals display a reduction in leptin-induced STAT3 phosphorylation in the NG, associated with a decrease in CCK-induced satiety [12]. This loss of satiety signaling may result in excessive consumption of calories, or hyperphagia. Interestingly, an acute high dose of LPS has been shown to have the opposite effect and promote anorexia. Acute LPS (100mg/kg) has *in vivo* and *in vitro* been found to induce inducible nitric oxide synthase (iNOS) leading to nitric oxide (NO) production [58]. NO can inhibit orexigenic neurons signaling at the level of the hypothalamus promoting anorexia [59, 60]. Similarly to leptin, iNOS signaling involved STAT3 recruitment. Interestingly repeated LPS exposure fails to induce STAT3 phosphorylation in the arcuate

nucleus of the hypothalamus and fails to induce anorexia suggesting that along with doses, chronic repeated exposure to LPS may be key in promoting intake [60].

In addition to impaired vagal signaling, there is evidence that bacteria-driven inflammation may alter vagal innervation. We have found in male rats that diet-induced dysbiosis is associated with a decrease in isolectin B4 (IB4)-positive fibers in the NTS [6]. IB4 is expressed by unmyelinated c fibers which are majority of vagal origin at the NTS level [61]. A reduction in vagal innervation to the brainstem is induced by both HFD and HSD and may result in impaired vagal function [62]. Vagal remodeling has previously been observed after vagal injury induced by vagotomy or capsaicin [62]. Central nervous system (CNS) resident parenchymal myeloid cells or microglia are recruited in response to injury, and chronic microglia activation can alter neuronal function [63]. In our studies, both HFD and HSD-induced dysbiosis were accompanied by an increase in microglia activation in the NG [6]. Additionally, we have found in male rats that administration of a broad spectrum antibiotic, minocycline, normalized HFD-induced dysbiosis, microglia activation and vagal remodeling as well as hyperphagia [13]. This data supports the idea that microbiota-driven microglia recruitment may promote vagal rewiring, potentially altering vagal satiety signaling and regulation of food intake. Interestingly, diet content has been shown to improve vagal sensitivity to CCK. For example, A recent study investigating the effect of HPD in male rats found that microbiota changes were accompanied by an increase in CCK sensitivity [30].

LPS is not the only pro-inflammatory bacterial product released by a dysbiotic microbiota, however its mode of action is the best studied. Flagellin and peptoglygan productions from gut bacteria also increase diet-induced dysbiosis. Peptoglycan signals via the vagus nerve as peptoglycan-induced locus coeruleus (LC) neurons excitation is blunted by sub-

diaphragmatic vagotomy in female Wistar rats [64] . This study found comparable vagally-mediated effect of LPS on the LC neurons, showing similarities in LPS action between male and female rats.

Deleterious effects of diet-induced dysbiosis may also be related to a decrease in beneficial bacterial products, notably SCFA. In addition to their trophic role mentioned previously, SCFAs promote anorexigenic gut peptides secretion, especially GLP-1, via G protein–coupled receptors FFAR2 and FFAR3 activation on L cells [40]. Interestingly, FFAR3 is also expressed in the enteric nervous system, including on capsaicin-sensitive sensory neurons [65] and FFAR3 activation on portal nerves increase neuronal activity in the dorsal vagal complex [65]. In addition, SCFA have immunomodulatory properties and have been found to regulate microglia function in the CNS of male and female mice via a FFAR2-dependent pathway [66]. Finally, bacteria may also directly signal to the brain via release of neurotransmitters such as dopamine, serotonin, acetylcholine, γ-aminobutyric acid, and tryptophan [67] but these pathways have not yet been explored in relation with eating behavior.

Perspectives and Significance

Composition of the gut microbiota is ever-changing in relation to diet composition, timing of eating, and other environmental factors. In HFD models, gut microbiota dysbiosis initiates inflammatory responses and diminishes intestinal barrier function, allowing bacterial products into circulation. Chronic, low-grade inflammation is associated with a decrease in gut peptide signaling sensitivity, hyperphagia and weight gain. Microbiota-driven microglia recruitment may be involved in diet-driven loss in vagally-mediated satiety. An exciting new avenue of research in this field has focused on understanding the exact influences of various glial cells and how they interact with vagal neurons. Identifying the specific signaling molecules and

mechanisms that drive vagal remodeling is essential to increase understanding of the microbiota-gut-vagal-brain interaction. Further investigation into these pathways' may be an important step in developing effective clinical treatments of obesity and other disorders. However, there are still hurdles and unknowns, especially related to microbiota manipulation.

First, as diet composition is a major regulator of gut microbiota composition [10], many interventions manipulate diet composition to change the bacterial make up. Although this is effective in achieving the desired microbiota composition, it makes differentiating between diet-induced changes and microbiota-induced changes difficult. This can be overcome by the use of a germ-free animal model. However, germ-free animals have lowered immune systems, altered GI morphology, neuroanatomy, and other significant differences when compared to their conventional counterparts [68]. The stability and durability of microbiota manipulation is also relatively unknown. The majority of the current research has focused on weight gain prevention in response to a HFD challenge but it remains undermined if microbiota manipulation is a viable tool for weight loss. Particularly in humans, where if bad dietary habits are maintained, one would expect dysbiosis to settle again. It should be noted that in mice, microbiota transfer appears to have effects up to 17 weeks post- colonization, which is a relative long term effect considering the lifespan of the animals (2-3 years) [69].

Finally, the overwhelming majority of the research on microbiota-host behavior has been conducted in male subjects. Chronic inflammatory conditions that may be related to microbiota dysbiosis, such as autoimmune disorders, often are sexually dimorphic. There are reported sex differences in microbiota composition [70], yet the female bug-gut-brain axis has been understudied.

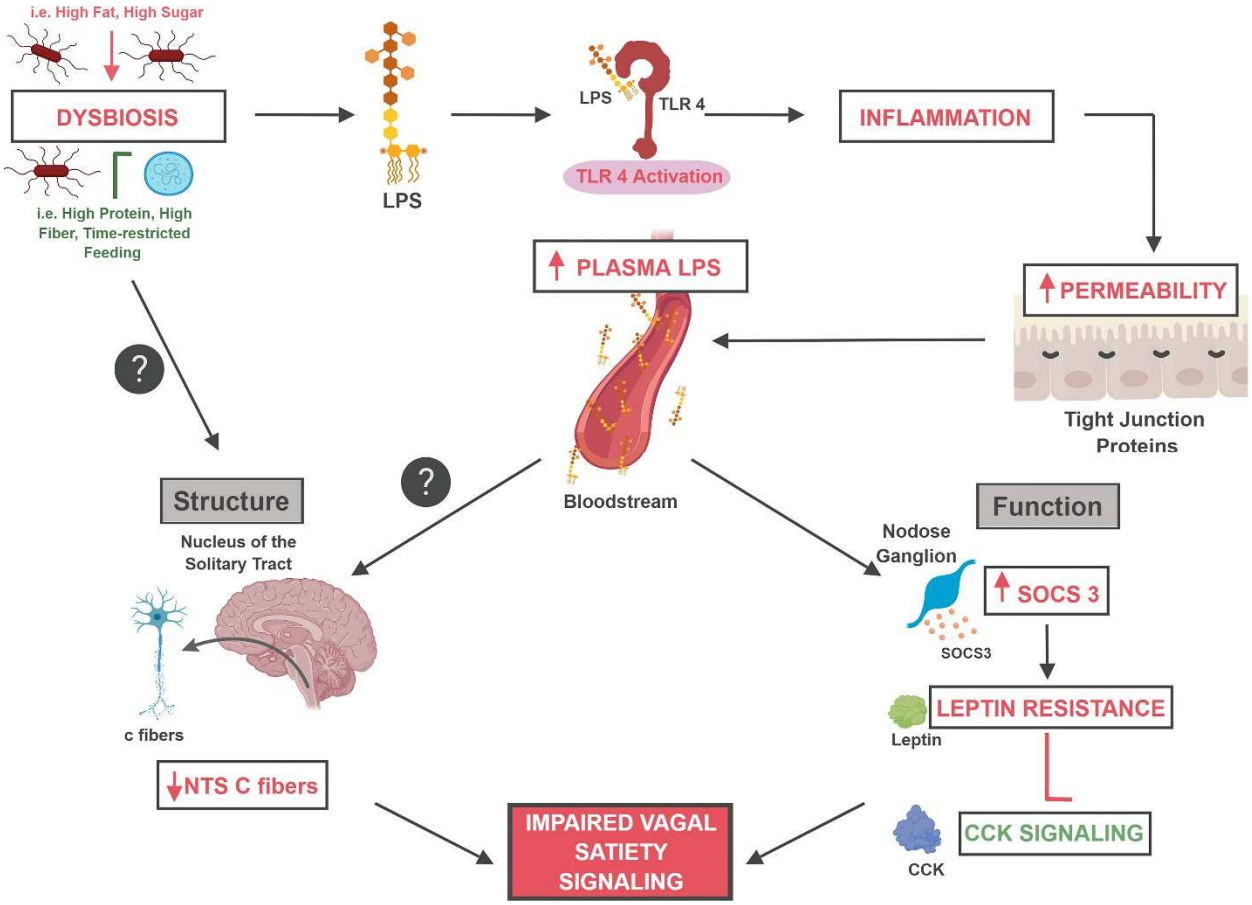

FIGURE 1.1. Graphical summary. Graphical summary depicting the potential pathways by which microbiota-driven inflammation can influence the gut-brain axis to modulate ingestive behavior.

CHAPTER 2

POTATO-RESISTANT STARCH SUPPLEMENTATION IMPROVES MICROBIOTA DYSBIOSIS, INFLAMMATION, AND GUT-BRAIN SIGNALING IN HIGH FAT-FED RATS[2]

[2] Adapted from Klingbeil EA, Cawthon C, Kirkland R, de La Serre CB. Potato-Resistant Starch Supplementation Improves Microbiota Dysbiosis, Inflammation, and Gut-Brain Signaling in High Fat-Fed Rats. Nutrients. 2019;11(11):2710. Reprinted here with permission of publisher.

Abstract

Background: High-fat (HF) diet promotes gut microbiota dysbiosis, which is associated with systemic inflammation. Bacterial-driven inflammation is sufficient to alter vagally mediated satiety and induce hyperphagia. Promoting bacterial fermentation improves gastrointestinal (GI) epithelial barrier function and reduces inflammation. Resistant starch (RS) escape digestion and can be fermented by bacteria in the distal gut. Therefore, we hypothesized that potato RS supplementation in HF-fed rats would lead to compositional changes in microbiota composition associated with improved inflammatory status and vagal signaling.

Methods: Male Wistar rats (n = 8/group) were fed a low-fat chow (LF, 13% fat), HF (45% fat), or an isocaloric HF supplemented with 12% potato RS (HFRS) diet.

Results: The HFRS-fed rats consumed significantly less energy than HF animals throughout the experiment. Systemic inflammation and glucose homeostasis were improved in the HFRS compared to HF rats. Cholecystokinin-induced satiety was abolished in HF-fed rats and restored in HFRS rats. HF feeding led to a significant decrease in positive c fiber staining in the brainstem which was averted by RS supplementation.

Conclusions: RS supplementation prevented HF diet induced gut dysbiosis and systemic inflammation. Additionally, microbiota manipulation via dietary potato RS prevented HF-diet-induced reorganization of vagal afferent fibers, loss in CCK-induced satiety, and hyperphagia.

Keywords: gut microbiota; resistant starch; inflammation; glucose tolerance; vagal nerve; obesity

Introduction

Prevalence of obesity has soared to 93.3 million people in the United States [1]. Obesity has been characterized as a low-grade inflammatory state, and inflammation plays a critical role in both the exacerbation of obesity and the development of co-morbidities such as diabetes [2].

There is accumulating evidence that the chronic low-grade inflammation characteristic of obesity is at least partially controlled by the gut microbiota [3]. The gastrointestinal (GI) tract is home to over 10^{14} microorganisms, primarily bacteria, and microbiota makeup can influence host physiology and behavior [4]. Microbiota composition changes with diet and is especially responsive to/can be modulated by dietary fats [5,6], sugars [7], and fibers [5,8]. An abnormal microbiota composition, or dysbiosis, has been associated with increased adiposity in both humans [9,10] and animal models [7,11]. Obesity-associated microbiota is characterized by an increase in its pro-inflammatory potential [12,13] Additionally, dysbiosis alters GI epithelial barrier function, allowing bacterial by-product to exit the gut into the circulatory system [6,13,14]. Chronic administration of pro-inflammatory bacterial lipopolysaccharide (LPS) is sufficient to increase food intake [15] and induce weight gain [15,16] and insulin resistance [16], showing a direct relationship between bacterial products and development of obesity and associated comorbidities.

The GI microbiota composition can alter gut–brain communication, potentially affecting vagally-mediated post-ingestive feedback and intake regulation. Gut originating satiety signals, such as cholecystokinin (CCK), are released in response to feeding and act on vagal afferents to promote meal termination [17]. Animals fed high-fat (HF) or high-sugar diets displayed marked dysbiosis associated with reduction in isolectin B4 (IB4)-positive fibers at the level of the nucleus of solitary tract (NTS) where vagal afferents terminate [7]. Isolectin B4 binds to unmyelated c-fibers which, in the medial NTS, are predominantly of vagal origin [18]. Gut–brain vagal

remodeling may be linked to bacterial-driven inflammation as antibiotic administration in HF-fed rats normalizes microbiota composition, NTS IB4 staining, and the accompanying immune cells activation observed in the NTS [19].

In addition, to effects on energy homeostasis, chronic inflammation can promote the development of metabolic disorders, especially insulin resistance. Pro-inflammatory cytokines, such as tumor necrosis factor (TNF)-α and interleukin (IL)-1β, can promote insulin receptor substrate-1 (IRS1) phosphorylation at serine 307 (p-IRS1, Ser307), inhibiting insulin action [20,21].

Preventing dysbiosis and/or preserving the gut epithelial barrier integrity may inhibit systemic inflammation and prevent weight gain and insulin resistance. Treatments with prebiotics [16] and antibiotics [22] can restore epithelial barrier function. In humans, prebiotic supplementation has been associated with an increase in markers of bacterial fermentation [23]. Short-chain fatty acids (SCFAs) are the main products of bacterial fermentation; acetate, propionate, and butyrate are the predominant SCFAs found in the intestine [24]. Short-chain fatty acids stimulate the production and differentiation of enterocytes, improving mucus production and epithelial health [25,26]. In animal models, supplementation with soluble fibers increases SCFA production, decreases inflammation, and positively affects glucose homeostasis [16,22,27].

Similar to fibers, resistant starch (RS) is a naturally occurring compound that escapes digestion in the proximal gut and can reach the distal GI (ileum and colon) and be fermented by gut microbiota [28,29]. Starch can resist digestion due to the fact of entrapment within a food (RS_1), their chemical structure (RS_2), or retrogradation during cooking (RS_3) [28]. In humans, supplementation with RS has been shown to increase fecal SCFA [28]. Consumption of RS_2 enhances acetate production, and RS_3 increases propionate production [28]. There is evidence that

RS consumption is associated with positive health outcomes: in piglets, supplementation with 10 g/day of potato starch improves insulin resistance [30], while in humans, corn RS consumption (24 g/d) is associated with lower fasting glucose levels [31]. Additionally, maize RS_2 supplementation in rodents has been shown to alter gut microbiota composition [32] and improve inflammatory status [33].

Americans consume on average 4.9 g of RS daily [34]. Among commonly consumed foods, potatoes are a good source of RS, providing 2 to 5 g of RS per 100 g. The RS contents in potatoes vary with cooking method and temperature but are fairly constant among commonly consumed varieties of potatoes [35]. Raw potatoes are particularly rich in RS_2; potato starch granules contain highly phosphorylated amylopectin and amylose that are not easily hydrolyzed [36]. Higher amounts of RS in raw potatoes have been shown to increase digestion time, potentially providing similar benefits as fermentable fibers [29].

There is limited knowledge on the potential protective effects of potato RS supplementation on gut microbiota composition, inflammatory status, and gut–brain signaling in diet-induced obesity models. In this study, we hypothesized that potato RS supplementation would prevent the onset of diet-driven microbiota dysbiosis, preserving gut–brain communication and preventing weight gain and metabolic dysfunctions associated with HF feeding.

Methods

Animals and Diets: Twenty-four male Wistar rats were procured from Envigo (Indianapolis, IN, USA) and single-housed in wired-hanging cages in a temperature-controlled animal facility with a 12 h light–dark cycle. Following three days of habituation, animals were divided into three groups (n = 8 per group) and fed either a regular control chow diet (13% kcal from fat), HF diet (45% kcal from fat), or a HF diet supplemented with potato RS (HFRS) for 8

weeks. Animals were randomly assigned to groups and there were no differences in body weight at baseline among groups.

The chow control diet was ordered from Lab Supply (Fort Worth, Texas, PicoLab (5053), USA). The HF and HFRS diets were custom-made by Research Diets (New Brunswick, NJ, USA) and matched for energy density, macronutrient, and fiber contents (Table 1). The cornstarch and a portion of the maltodextrin in the 45% fat HF diet (D12541) were replaced with raw, unmodified potato starch in the HFRS diet (D17101605) (Bob's Red Mill, Milwaukie, OR, WI, USA). Calculations were originally made based on the assumption that raw potato starch contains 50% RS [37]. Energy density for RS was calculated at 2.8 kcal/gram [38]; energy density for the 50% digestible portion of the potato starch was estimated at 4 kcal/gram. To make up for the lower overall energy density of the potato starch powder, maltodextrin contents were increased in the HFRS diet **(Table 2.1).** The HFRS diet was designed to contain 10% potato RS; this supplementation dose was based on previous data from our lab [27] and past research [39]. We verified the RS contents of the raw potato starch using a commercially available assay (Megazyme, Chicago, IL, USA) and determined that Bob's Red Mill potato starch contains approximately 60% RS **(Supplementary Table S2.1 and S2.2)**, bringing our final supplementation level to approximately 12% and the HFRS energy density to 4.6 kcal/g **(Table 2.1).**

After 8 weeks on their respective diets, animals were fasted for 2 h and euthanized via CO_2 inhalation. The sacrifice order was evenly distributed among groups and all tissues were collected within 6 h of light onset. Blood was sampled by cardiac puncture and rested on ice for 30 min before centrifugation at 4 °C at 8000 rpm for 10 min for serum collection. The GI tissues (i.e., duodenum, ileum, cecum, and feces) and visceral fat pad were collected, snap frozen, and stored at −80 °C. Brains were extracted and immediately placed in 4% paraformaldehyde solution (PFA)

until brains sunk to the bottom of the tubes. Brains were then moved into 30% sucrose solution for cryoprotection. All animal care procedures were approved by the Institutional Animal Care and Use Committee of the University of Georgia, AUP A2017 08-017-R2.

Food Intake and Body Weight: Body weight and food intake were measured 3 days a week at the beginning of the light cycle for the entirety of the 8 week feeding intervention. Food intake (g) was determined by subtracting the amount of the remaining diets in the cages from the amount previously provided. Animals were housed in wired, hanging cages to ensure that food spillage was included.

Gut Microbiota and SCFA Quantification: Fecal pellets were collected at day 0 and after 8 weeks on the respective diets. Bacterial DNA were extracted from samples using the ZR Fecal DNA MiniPrep kit per the manufacturer's protocol (Zymo Research, Irvine, CA, USA). The V4–V6 region of the 16S rRNA gene was amplified with the following primers: F515 (5'-GTGCCAGCMGCCGCGGTAA -3') and RNextera (5'- CGACRRCCATGCANCACCT -3') and targeted for sequencing by Ilumina MiSeq (University of Georgia Genomics Facility). Bacterial 16S sequences were processed with QIIME. The OTUs were picked based on 97% sequence similarity via the UCLUST algorithm. The OTUs were assigned to taxa through the Greengenes database. Chao index was calculated to determine α-diversity. The METAGEN assist platform was used to assess β-diversity. Taxonomic abundances were log transformed for non-parametric tests. Multivariate analysis was conducted using the Galaxy platform linear discriminant analysis effect size (LEfSe) to identify taxonomic features discriminating of one or more groups. The SCFAs in fecal samples were quantified using gas chromatography mass spectrometry at Mayo Clinic Laboratories (Rochester, MN, USA) as previously described [40].

GI Function:GI Morphology and Goblet Cell Proliferation: Sections of distal small intestine (ileum) were cryosectioned (8 μm, Leica CM1900, Leica Biosystems, Wetzlar, Germany) and stained with alcian blue and nuclear fast red (Sigma–Aldrich, St. Louis, MO, USA). Villus length and the number of goblet cells (per crypt) were measured manually in well-oriented sections (5 measurements per ileal section) using a light microscope (BX40, Olympus) equipped with a digital camera (DP25, Olympus) and analysis software (DP2-BSW, Olympus).

GI Permeability: Circulating LPS levels were measured as a proxy for intestinal barrier integrity. They were determined in serum using a pyrochrome lysate mix, a quantitative chromogenic reagent, diluted in Glucashield buffer which inhibits cross-reactivity with (1→3)-β-D-Glucans (Associates of Cape Cod, East Falmouth, MA, USA). Samples were diluted 1:10 in pyrogen-free water and heated for 10 min at 70 °C. Samples and reactive solution were incubated at 37 °C for 30 min, and absorbance was read at 405 nm on a Spectramax microplate reader (Molecular Devices, Sunnyvale, CA, USA).

Real-Time PCR: The mRNA was extracted from ileum samples using the RNeasy Mini Kit (Qiagen, Valencia, CA, USA). The cDNA was synthesized using the RevertAid First Strand cDNA Synthesis Kit (Thermo Fisher Scientific, Franklin, MA, USA). The RT-PCR was run on a StepOnePlus real-time PCR system (Thermo Fisher Scientific) using SYBR Green PCR master mix (Thermo Fisher Scientific) and GLP-1 and Muc2 primers purchased from Integrated DNA Technologies (Table S3). Data were analyzed according to the $2^{-\Delta\Delta Ct}$ method [41].

Sensitivity to Satiety Peptide CCK: After 6 weeks on their respective diets, animals were fasted for 12 h before receiving an administration of CCK (i.p., 0.22 nml/kg, Bachem, Torrance, CA, USA) or saline (i.p., 400 μl, vehicle). A control experiment was conducted in which rats did not receive any injections. Food intake was measured 30, 60, and 120 min post-injection.

Glucose Homeostasis: Oral Glucose Tolerance Test: After 7 weeks on respective diets, rats were fasted for 5 hours before oral gavage of 20% glucose solution (2 g/kg body weight). Glycemia was measured using a glucometer (Freestyle, Alameda, CA, USA) before oral gavage (0 min) and 15, 30, 60, 90, and 120 minutes after. Blood samples were collected at each time point and centrifuged as described above for insulin, glucagon, and GLP-1 analysis by multiplex ELISA (Meso Scale Diagnostics, Rockville, Maryland, USA).

Serum Inflammatory Markers: Serum collected at sacrifice was frozen at −80 °C and inflammatory markers were assessed using the FirePlex Rat Inflammation Immunoassay Panel (Abcam, Cambridge, MA, ab235665) by the Abcam Fireplex Service Lab.

Immunhistochemistry: Hindbrains were cryosectioned (20 μm, Leica CM1900 from the caudal to the rostral region of the NTS (between bregma −14.16 and −12.93 mm). Sections were stained for IB4 (Novus Biologicals, Littleton, CO, USA) to visualize unmyelinated c-fibers and for ionized calcium binding adaptor molecule 1 (IBA1, Wako Chemicals, Richmond, VA, USA) which stains microglia.

After blocking with 10% goat serum in phosphate buffered saline (PBS), sections were incubated with primary antibody against IBA1 or with IB4 biotin conjugated overnight at 4 °C. Negative controls received 10% goat serum in PBS instead of primary antibody. Following washing, sections were incubated with secondary Goat anti-Rabbit IgG Alexa Fluor 488 conjugate (Invitrogen, Carlsbad, CA, USA) or ExtrAvidin-Cy3 (Sigma–Aldrich, St. Louis, MO, USA) for 1 h at 37 °C. Sections were mounted with fluoro gel (Electron Microscopy Sciences, Hartfield, PA, USA). Images of the NTS were captured at 20× magnification and stitched via a Nikon 80i imaging photomicroscope (Nikon, Tokyo, Japan) with a Nikon Digital Sight DS-Qi1Mc digital camera and filters for Alexa 488 and Extravidin-CY3. The IB4 and IBA1 fluorescence positive staining was

quantified at the level of the area postrema as previously described [7] using binary imaging analysis based on principles described in Reference [42]. Analysis was completed using the Nikon Elements AR 3.0 Imaging software (Nikon).

Statistical Analyses: Unless stated otherwise (microbiota analyses), statistical analyses were performed using Prism software (Prism 6.0; GraphPad Software, La Jolla, CA, USA). Two-way repeated measures ANOVA was used to analyze body weight, energy intake, and OGTT with Tukey's post-hoc test. One-way ANOVA was performed to analyze biochemical analyses. Non-normal datasets were analyzed with non-parametric methods. Differences were considered significant if $p < 0.05$. Data are presented as the mean ± SEM.

Results

Potato RS Reduces Weight Gain and Prevents Hyperphagia: The HF fed animals gained significantly more weight than the chow control group over the course of the study **(Figure 2.1A).** They weighed significantly more starting at week 2 (chow 303.1 ± 6.8 g versus HF 334.7 ± 10.3 g, $p < 0.05$) and stayed heavier throughout the rest of the study. The RS supplementation led to a significant reduction in weight gain (HF 492.1 ± 16.2 g versus HFRS 445.1 ± 12.2 g, $p < 0.01$) but did not fully prevent a diet-induced increase in body weight as HFRS rats still weighed significantly more than the chow-fed control animals (chow 397.5 ± 6.7 g versus HFRS 445.1 ± 12.2 g, $p < 0.01$).

The HF-fed rats consumed more kcal than the chow control group for the entire duration of the study **(Figure 2.1B)** with the exception of week 2. The RS supplementation led to a significant decrease in diet-induced hyperphagia. The RS-supplemented rats initially displayed hyperphagia when first exposed to the diet (chow 82.6 ± 0.8 versus HFRS 93.76 ± 2.7 kcal/day, $p < 0.001$), although this first hyperphagic phase was significantly reduced compared to the HF

group (HF 105.2 ± 5.3 versus HFRS 93.76 ± 2.7 kcal/day, $p < 0.001$). Throughout the rest of the experiment, the HFRS-fed rats' intake was fairly similar to the chow-fed animals' intake with the exception of week 4 (chow 84.3 ± 2.0 versus HFRS 91.5 ± 3.6 kcal/day, $p < 0.05$). Overall, over the 8-week period, HF rodents consumed significantly more kcal in total than either chow or HFRS rats **(Figure 2.1C)** (HF 2652 ± 295 versus chow 2260 ± 105 kcal, $p < 0.01$ and versus HFRS 2373 ± 216 kcal, $p < 0.05$). While chow and HFRS rats' intake did not significantly differ ($p = 0.56$).

Potato RS Improves HF Diet-Driven Microbiota Dysbiosis: The HF-fed rats displayed an overall dysbiotic microbiota profile that was significantly different from the chow-fed rats **(Figure 2.2 and Supplementary Figure S2.1).** The HF feeding led to marked changes in microbiota composition, characterized by an increase in the Firmicutes:Bacteriodetes ratio (chow 2:1 versus HF 8.6:1) and abundances of *Clostridia* (chow 54.28 ± 3.2 versus HF 76.18 ± 1.9, $p < 0.0001$). The increase in *Clostridia* abundances was driven by a bloom in families *Dorea* ($p < 0.001$) and *Peptococcaceae* ($p < 0.001$). The LEfSe showed that the Firmicutes classes *Clostridia* and *Erysipelotrichi* were characteristic of HF fed rats, in particular the order *Clostridiales* (Family, *Dorea*) and *Erysipelotrichiales* (Family, *Erysipelotrichaceae*) **(Figure 2.2E).**

Potato RS supplementation normalized the *Firmicutes:Bacteriodetes* ratio (HF 8.6:1 versus HFRS 1.7:1) along with reductions in the abundance of class Clostridia (HF 76.18 ± 1.9 versus HFRS 38.70 ± 7.3, $p < 0.001$) and the genera *Lactococcus* ($p < 0.01$), *Facklamia* ($p < 0.05$), *Peptococcus* ($p < 0.05$), *Dorea* ($p < 0.05$), and *Rothia* ($p < 0.05$). The RS supplementation also normalized abundances of Bacteroidetes ($p < 0.001$), particularly *Prevotella* ($p < 0.001$). The RS supplementation led to a significant increase in Actinobacteria ($p < 0.001$) abundances compared to both chow-fed control and HF-fed rats. Probiotics *Bifidobacterium* are Actinobacteria, and RS supplementation specifically increased abundances of genera *Bifidobacterium* ($p < 0.01$) and

Collinsella ($p < 0.01$). The LEfSe showed that Actinobacteria, in particular *Bifidobacterium,* were particularly characteristic of the HFRS-fed rats **(Figure 2.2).** Overall profile cluster analyses and PCA determined a strong relationship between diet and microbiota profile composition. Analysis at all taxa levels determined significant differences among all three diet groups **(Figure 2.2A,B),** with the strongest differences between the HF and HFRS groups. Potato RS supplementation resulted in a microbiota composition more closely related to chow than HF **(Figure 2.2A,B,C)** and a specific increase in *Bifidobacterium spp*.

Potato RS Increases Fecal SCFA Content: The HF feeding led to a significant decrease in fecal acetate contents compared to the chow diet (chow 198.3 ± 12.8 versus HF 55.9 ± 5.9 nmol/5 g feces, $p < 0.0001$) and fecal propanoic acid contents (chow 47.3 ± 6.7 versus HF 6.2 ± 1.2 nmol/5 g feces, $p < 0.01$). The RS supplementation prevented an HF diet-driven decrease in acetate (HFRS 202.3 ± 26.1 nmol/5 g versus HF, $p < 0.0001$, versus chow, $p = 0.77$) and propionate (HFRS 51.2 ± 10.5 nmol/5 g versus HF, $p < 0.001$, versus chow, $p = 0.77$). Lastly, chow feces contained significantly more butyric acid than the HF animals (chow 52.3 ± 7.0 versus HF 6.6 ± 1.3, $p < 0.01$) and HFRS animals (chow 52.3 ± 7.0 versus HFRS 19.9 ± 4.4, $p < 0.05$) **(Figure 2.2D).**

Potato RS Attenuates Hypertrophy and Inflammation: The HF feeding led to a significant increase in villus height compared to the chow control group (chow 476 ± 24.3 versus HF 667 ± 19.8 μm, $p < 0.0001$). The RS supplementation partially normalized villus height **(Figure 2.3A).** Villi high in the ileum of HRS-fed rats were significantly reduced compared to HF-fed animals ($p < 0.05$) but sill significantly higher than chow-fed rats ($p < 0.01$). There were no differences in goblet cell counts among the groups.

Serum LPS levels were elevated in the HF-fed rats compared to the chow control animals **(Figure 2.3B)** (chow 0.33 ± 0.07 versus HF 0.56 ± 0.08, $p = 0.016$). This was normalized by RS supplementation. Serum TNFα levels in HF animals were significantly elevated compared to the chow control **(Figure 2.3C)** (chow 2.22 ± 0.19 versus HF 3.93 ± 0.59 pg/mL, $p < 0.01$). This was partially reduced by RS supplementation (HF versus HFRS 2.95 ± 0.25, $p = 0.1$). Similarly, serum IL-6 levels were significantly increased in the HF animals (chow 1.41 ± 0.32 versus HF 3.45 ± 0.58 pg/mL, $p < 0.01$) and this was normalized in the HFRS rats (HF versus HFRS 1.84 ± 0.26 pg/mL, $p < 0.05$) **(Figure 2.3F).** Interestingly, serum IL-10 levels were significantly elevated in the chow animals compared to both HF (chow 7.6 ± 0.62 versus HF 5.0 ± 0.27 pg/mL, $p < 0.01$) and HFRS (chow versus HFRS 5.7 ± 0.46, $p < 0.05$) **(Figure 2.3D).** Serum IL-1B levels were not significantly different among groups **(Figure 2.3E).**

Potato RS Improves Glucose Tolerance: An OGTT was conducted after 7 weeks on the respective diets. There was a significant increase in baseline glycemia in both HF- and HFRS-fed rats compared to chow-fed controls **(Figure 2.4A).** Glycemia increased in all groups following an oral glucose challenge and stayed elevated throughout the sampling period. The HF and HFRS glycemia was significantly higher than the chow control group at 15, 30, 45, and 60 min post challenge. The HFRS rats recovered faster than HF rats from this high glycemic episode, and the HFRS rats' circulating glucose levels were significantly lower than HF-fed rats at 90 and 120 min post challenge (90 min HF 159.1 ± 11.4 versus HFRS 139.7 ± 4.1 mg/dL, $p < 0.05$ and 120 min HF 144.2 ± 11.0 versus HFRS 123.2 ± 4.0 mg/dL, $p < 0.01$) but stayed elevated compared to the chow control rats (90 min chow 112.9 ± 6.2 mg/dL versus HFRS, $p < 0.001$ and 120 min chow 104.4 ± 1.5 mg/dL versus HFRS, $p < 0.05$). The overall glycemic response (area

under the curve, AUC) was significantly altered in HF-fed rats which was partially but not fully improved by RS supplementation **(Figure 2.4A,B).**

Insulin levels were increased in all groups in response to the glucose challenge. Insulinemia peaked at 15 min post gavage. Insulin levels in HF-fed rats were significantly higher than in the chow control group at 15 (chow 683 ± 201 versus HF 2597 ± 330 pg/mL, $p < 0.0001$) and 30 min (chow 542 ± 91 versus HF 1711 ± 247 pg/mL, $p < 0.0001$). The RS supplementation normalized glucose-induced insulin release; there were no significant differences in insulinemia between the HFRS rats and chow animals throughout the OGTT time course **(Figure 2.4C,D).** Lastly, GLP-1 levels were measured in serum collected at sacrifice, and HF-fed rats displayed significantly reduced circulating GLP-1 levels compared to chow animals (chow 16.2 ± 0.9 versus HF 10.1 ± 0.8 pg/mL, $p < 0.01$); this was normalized by RS supplementation **(Figure 2.4E).**

Potato RS Prevents HF Diet-Driven Loss in CCK Satiety: A CCK-sensitivity test was conducted after 6 weeks on respective diets. After a 12 h fast, food intake was recorded for 2 h following no injection (control) or an i.p. injection of saline (400 µl) or CCK (0.22 nmol/kg). For all groups, there were no significant differences in food intake between control and saline injection conditions (data not shown). In chow-fed rats, CCK injections led to a significant reduction in food intake compared to the saline conditions (saline 9.6 ± 0.3 versus CCK 7.9 ± 0.6 g, $p < 0.05$). This CCK-induced satiety response was lost in HF-fed rats; animals consumed as much food when they administered CCK as when they received saline (saline 6.6 ± 0.4 versus CCK 6.6 ± 0.6 g, $p = 0.97$). RS supplementation prevented HF-diet driven loss in CCK-induced satiety; there was a significant reduction in intake following CCK administration compared to saline in HFRS rats (saline 8.8 ± 0.7 versus CCK 7.5 ± 0.5 g, $p < 0.05$) **(Figure 2.5).**

Potato RS Reduces NTS Microglia: We quantified IBA1-positive staining at the level of the medial NTS. The HF feeding led to a significant increase in IBA1-positive staining intensity in the NTS compared to HFRS (HF 0.065 ± 0.024 versus HFRS 0.011 ± 0.003, $p < 0.05$), but this did not reach significance when compared to chow controls (chow 0.025 ± 0.007 versus HF, $p = 0.127$) **(Figure 2.6).** Increased intensity of IBA1 revealed a seemingly increased microglia presence and/or activation in HF animals whereas RS supplementation attenuated this neuroinflammatory response **(Figure 2.6).**

Potato RS Prevents Vagal Remodeling: We quantified IB4-positive staining at the level of the medial NTS. The HF diet significantly reduced IB4 staining in the NTS compared to the chow control (chow 0.37 ± 0.05 versus HF 0.06 ± 0.09 binary area fraction, $p < 0.0001$). Potato RS prevented the diet-induced loss in c-fibers positive staining. There was significantly more IB4 positive fluorescence in the NTS of HFRS rats compared to HF-fed animals (HF versus HFRS 0.35 ± 0.04 binary area fraction, $p < 0.001$). The c-fiber innervation in the NTS was comparable in the chow- and HFRS-fed rats **(Figure 2.7).**

Discussion

Our study found that potato RS supplementation reduced weight gain and prevented HF-diet-induced hyperphagia. Expectedly, RS supplementation improved microbiota dysbiosis and increased fecal SCFA content. Compared to HF rodents, the HFRS rats exhibited lower levels of inflammation. Functionally, the HFRS rodents improved glucose homeostasis, and RS supplementation prevented HF diet-driven loss in CCK satiety. For the CCK signals, predominantly through activation of the vagus nerve, we found that potato RS prevented vagal remodeling and recruitment of immune cells at the level of the NTS, potentially preserving vagally mediated satiety signaling.

Potato RS supplementation successfully attenuated weight gain associated with a HF diet. However, HFRS rodents gained significantly more weight than chow controls despite no overall differences in energy intake. While HFRS did consume more energy on a certain week, the difference in body weight may not be solely due to kcal intake. Other factors could include energy expenditure (which was not measured), microbiota composition and fecal energy harvest, and dietary macronutrient composition. Specifically, adiposity in rats has previously been shown to be proportional to dietary fat contents [43]. Additionally, HFRS rodents' meal patterns may also have been different from the chow-fed rats, which can influence body weight [44,45].

Potato RS supplementation led to a marked improvement in diet-driven microbiota dysbiosis. The microbiota is the community of commensal, symbiotic, and pathogenic microorganisms that coexist in the human body [46]. In the GI microbiota alone, there are more than 10^{14} bacteria and over 400 bacterial species [46]—more than 10 times bacterial cells than human cells. Ninety-five percent of the gut microbiota is composed of two major phyla: Firmicutes and Bacteroidetes [6,9,47]. In our study, the HF diet increased the Firmicutes:Bacteriodetes ratio, a consistent finding in response to a HF diet [47]. Within Firmicutes, the classes Clostridia and Erysipelotrichia bloomed in the HF-fed rats, while the abundances of the Bacteroidales (order, Bacteriodetes) were significantly decreased compared to chow-fed animals, again consistent with previous findings [7,27]. These changes were associated with a significant decrease in SCFA content in the feces of HF-fed rats.

Around 100–200 mmol of SCFAs are produced daily in the human colon [48]. Diets higher in insoluble fibers promote SCFA production by colonic anaerobic bacteria [48]. These microbiota-accessible carbohydrates—fructooligosaccharides, cellulose, and resistant starches—are degraded by "primary degraders", such as *Bifidobacterium* spp., *Bacteriodes* spp., and

Ruminococcus Bromii [49], and broken down into propionate, acetate, and glucose. In our study, we found that the microbiota of potato RS-supplemented rats were significantly enriched in *Bifidobacterium* spp. and Bacteroidale*s*, the order of bacteria containing the previously mentioned *Bacteriodes* spp. Previous studies have found similar increases in *Bifidobacterium* in response to fiber and/or RS supplementation [50–53]. These changes were associated with higher levels of SCFAs in the distal gut, particularly acetate and propionate. Interestingly, propionate and acetate have been shown to play opposite roles in hepatic lipogenesis. Propionate appears to prevent liver lipid accrual [54], while acetate promotes it [55]. Increased acetic acid levels in HFRS rats may explain the lack of differences in liver lipid levels between HFRS and HF rodents. Critical in gut health, SCFAs promote mucus secretions, cell survival, and tight junction proteins' integrity [56]. The HF-fed rats had significantly longer villi in the ileum than chow-fed animals. Increased villi length has been found with abnormal cell proliferation in GI disease states [57], supporting a decrease in gut function in HF-fed rats. The RS supplementation prevented HF diet-driven villi hypertrophy. Additionally, both acetate and propionate are activators of G-protein coupled receptors *ffar2* and *ffar3*, which increases peptide YY (PYY) and GLP-1 release when activated [58]. In our study, the HFRS rats displayed an increase in circulating GLP-1 compared to the HF-fed animals.

Improvements in gut function were associated with reduced systemic inflammation and improved glucose homeostasis in potato RS-supplemented rats. Diet-driven dysbiosis combined with impaired gut epithelial function allows for translocation of bacterial factors such as pro-inflammatory LPS to the circulation [13]. Chronic elevation in circulating LPS is sufficient to promote hyperphagia [15] and insulin resistance [23]. Notably, LPS promotes cytokines release [59]. In this study, RS supplementation decreased circulating serum levels of LPS and several pro-

inflammatory cytokines compared to HF-fed rats. This effect may be mediated via SCFAs, as propionate supplementation has been found to decrease LPS-induced inflammatory response [60]. Chronic inflammation is a key triggering factor in the development of insulin resistance; pro-inflammatory cytokines can notably impair insulin receptor substrate-1 (IRS-1) signaling [61]. As previously reported [62], a HF diet led to an increase in serum TNF-α which was reduced in HFRS rats ($p = 0.07$). IL-6 circulating levels were elevated in the HF-fed rats which was normalized in the HFRS animals. RS supplementation led to a decrease in the overall inflammatory tone which may explain why HFRS rats required less insulin to clear the same amount of glucose than the HF-fed rats. Increased circulating GLP-1 may also be linked to improved insulin sensitivity [63]. The GLP-1 receptor agonists have been found to decrease LPS-induced secretion of inflammatory cytokines such as TNF-α [64]. Positive effects of RS in glycemic control have been reported across species: RS supplementation in obese dogs is more effective in controlling glucose responses than soluble starches [65] and supplementation with RS has been shown to decrease fasting glucose, pro-inflammatory markers, cholesterols, waist circumferences, and percent body fat in humans with signs of metabolic syndrome [66].

Along with insulin resistance, bacterial inflammation also affects gut–brain signaling. Post-ingestive signals originating from the GI tract are relayed via the vagus nerve to the NTS to control meal size [67]. High-fat feeding alters gut–brain signaling resulting in overeating [68]. We previously found that chronic LPS administration is sufficient to impair vagally mediated satiety and increased intake [15], pointing toward a causal link between dysbiosis and diet-driven alteration in gut–brain communication. In addition to affecting vagal function, HF feeding leads to structural changes in vagal innervation. The vast majority of unmyelinated c-fibers at the level of the medial NTS level are of vagal origin [69] and can be labeled with IB4. The HF feeding leads

to a reduction in NTS IB4 staining [7], potentially affecting vagal function. Bacterial inflammation may play a key role in diet-driven vagal remodeling; a decrease in IB4 staining is accompanied by an increase in microglia recruitment along the gut–brain axis [70] and antibiotic administration prevents dysbiosis, microglia recruitment, changes in vagal structure, and hyperphagia in HF-fed rats [19]. Data from this study support a role for the microbiota in driving vagal maladaptation. Potato RS supplementation prevented diet-driven dysbiosis and maintained vagal NTS innervation pattern and sensitivity to gut satiety peptide CCK. Reduced sensitivity of post-ingestive negative feedback may explain the maintenance of hyperphagia in HF but not HFRS rodents [4].

Impaired vagal signaling may play a role in altering insulin release in response to glucose. Our results are consistent with previous studies that have found that HF diets increased serum insulin concentration immediately following glucose stimulus [71]. Interestingly, HF diet rats who underwent vagotomy prior to glucose tolerance test do not exhibit a large release of serum insulin [71].

Conclusion

Targeting the microbiota in obesity maybe an effective non-invasive therapeutic approach. Microbiota modulation through resistant starch supplementation, specifically from raw potato starch, may prove to be an effective preventive and treatment strategy for obesity through the development of functional foods. Composition of the gut microbiota is ever changing in relation to diet composition and other environmental factors. In HF diet models, gut microbiota dysbiosis decreases intestinal barrier function and initiates inflammatory responses. Increased SCFA production as a result of RS supplementation may attenuate the effects of a HF diet by improving gut barrier function, reducing systemic LPS levels, and increasing GLP-1 levels. Functionally, potato RS supplementation prevented hyperinsulinemia and maintained glucose homeostasis

compared to HF feeding alone. The RS supplementation also prevented diet-driven inflammation and remodeling of the gut–brain signaling, preserving vagally mediated satiety.

Table 2.1. Macronutrient composition of chow, HF, and HFRS as percent grams and energy.

	CHOW		HF		HFRS	
	Gram %	**kcal %**	**Gram %**	**kcal %**	**Gram %**	**kcal %**
Fat	4.5	13.1	24	45	23	45
Protein	20	24.5	24	20	23	20
Carbohydrates	53.5	62.4	41	35	43	35
Sucrose	3.2	3.2	20.1	17	20.1	17
Fiber	6	0	5.8	0	5.8	0
RS	1.4	0	0.1	0	11.9	0
Energy Density (kcal/g)	3.4		4.7		4.6	

Note: Maltodextrin was added to the HFRS diet to match energy density. Diets prepared by Research Diets, Inc. HF = high-fat diet, HFRS = high-fat resistant starch, RS = resistant starch, kcal = calories.

Supplemental Table S2.1. Diet composition of HF and HFRS diets[1]

Diet ingredient (g)	HF	HFRS
Casein	200	200
L-Cystine	3	3
Corn Starch	72.8	0
Maltodextrin 10	100	26
Raw Potato Starch[2]	0	172.8
Sucrose	172.8	172.8
Cellulose	50	50
Soybean Oil	25	25
Lard	177.5	177.5
Mineral Mix S10026	10	10
Dicalcium Phosphate	13	13
Calcium Carbonate	5.5	5.5
Potassium Citrate, 1 H2O	16.5	16.5
Vitamin Mix V100001	10	10
Choline Bitartrate	2	2
FD&C Yellow Dye #5	0	0
FD&C Red Dye #40	0.05	0
FD&C Blue Dye #1	0	0.05
Total	**858.15**	**884.15**

[1]Diets prepared by Research Diets, Inc. HF=high fat diet, HFRS=high fat resistant starch. [2] Potato starch was 60% resistant starch.

Supplemental Table S2.2. Resistant starch in raw potato starch, Chow, HF, and HFRS diets

	Potato Starch	Chow	HF	HFRS
% RS (g)	60	1.4	0.1	11.9

[1] HF, high fat; HFRS, high fat resistant starch; RS, resistant starch.

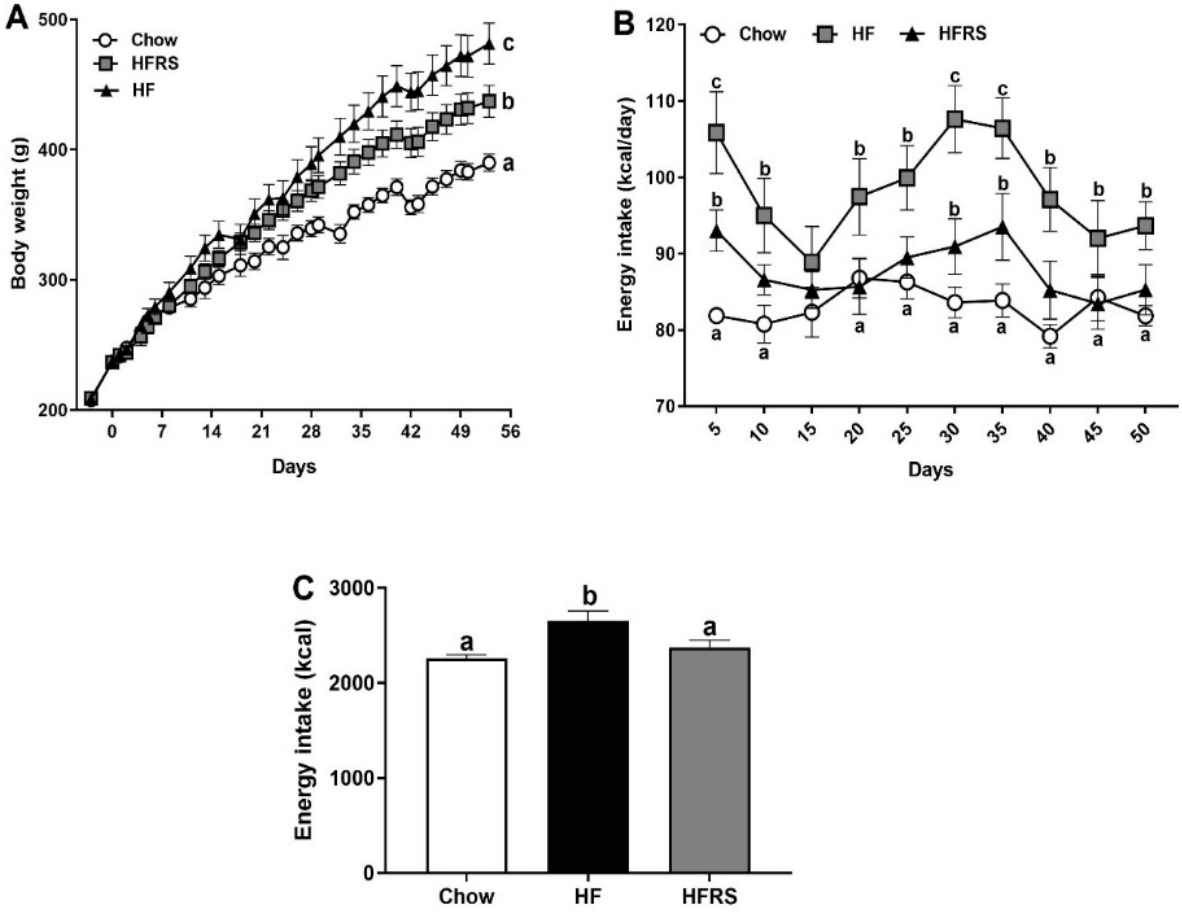

Figure 2.1. Potato RS reduces weight gain and prevents hyperphagia. (**A**) HF feeding led to a significant increase in body weight compared to control chow-fed conditions. The RS supplementation partially normalized weight gain. (**B**) The HF feeding led to a significant initial increase in energy intake in both HF and HFRS rats. The HF-fed rats' intake was significantly higher than chow-fed animals throughout the study with the exception of week 2. After initial hyperphagia, HFRS rats' energy intake normalized to the level of chow-fed rats, with the exception of week 4. (**C**) Overall energy intake was significantly higher in HF rats compared to both HFRS and chow control. Data are presented as the mean ± SEM; [a, b, c] different letters indicate statically significant ($p < 0.05$) differences among groups. HF = high fat, HFRS = high-fat resistant starch, $n = 8$ per group.

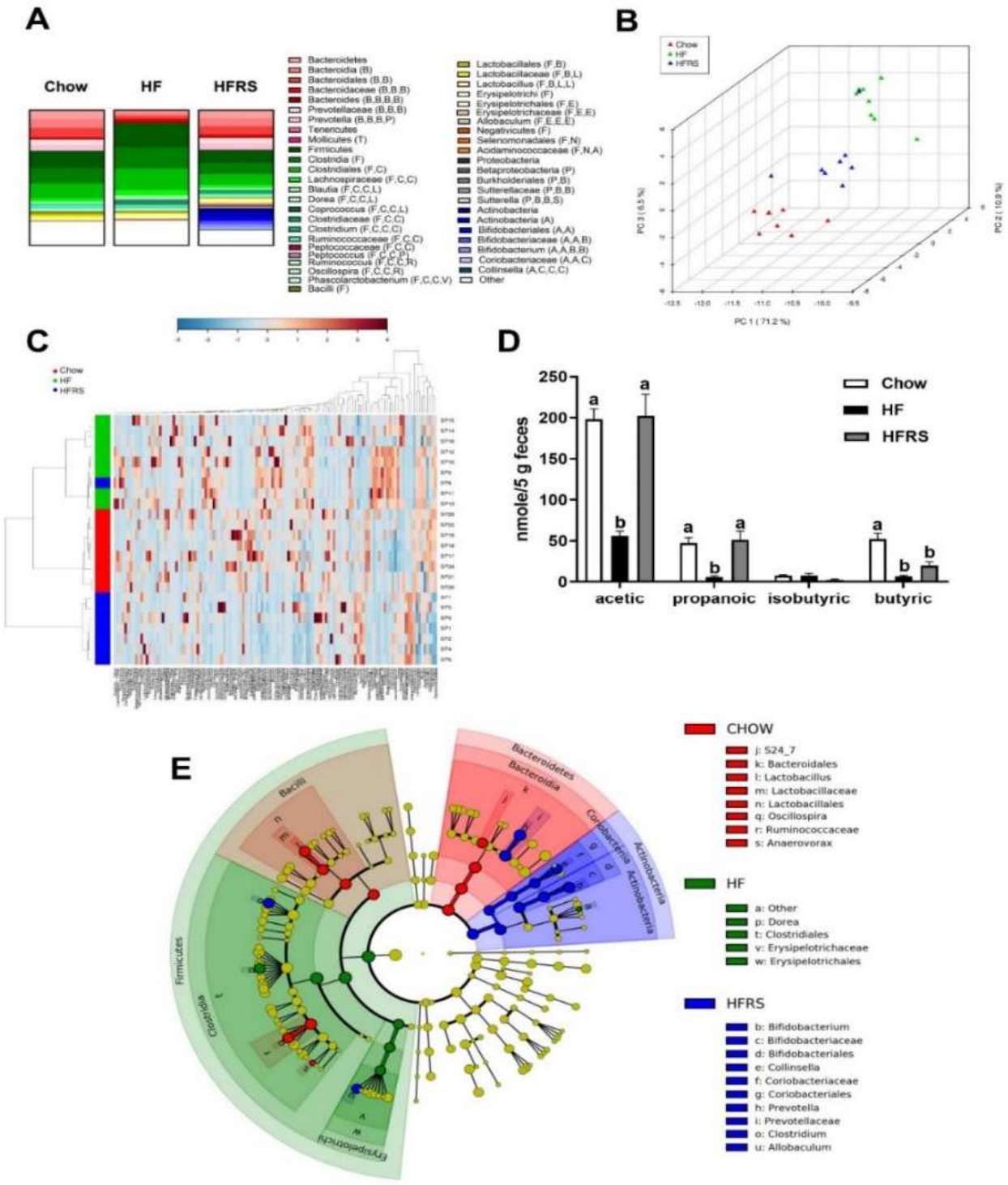

Figure 2.2. Potato RS improves microbiota dysbiosis. Microbiota abundance for chow, HF, and HFRS diet groups (**A**). The graph represents all abundances >1% at all phylogenic levels. Phyla: B: Bacteroidetes, F: Firmicutes, T: Tenericutes, P: Proteobacteria, A: Actinobacteria, V: Verrucomicrobia Class: B: Bacilli, B: Bacteroidia, C: Clostridia, E: Erysipelotrichia; M: Mollicutes, N: Negativicutes, D: Deferribacteres, A: Actinobacteria, V: Verrucomicrobiae, B: Betaproteobacteria. Order: B:

Bacteroidales, C: Clostridiales, L: Lactobacillales, E: Erysipelotrichiales, B: Burkholderiales, B: Bifidobacteriales. Family: C: Clostridiaceae, L: Lachnospiraceae, R: Ruminococcaceae, L: Lactobacillaceae, E: Erysipelotrichaceae, D: Desulfovibrionaceae, B: Bifidobacteriaceae, V: Verrucomicrobiaceae, (**A**): Acidaminococcaceae. *The* PCA plot (run with all phylogenic levels, 121 normalized taxa abundances) shows similarities in overall microbiota profiles between chow and HFRS, while HF-fed rats displayed a distinct microbiota profile (**B**). The metagene heat-map displays microbiota characteristics among diet groups (**C**). RS supplementation developed a significantly different microbiota profile than HF. RS supplementation significantly improved fecal SCFA content (**D**). GALAXY cladogram highlights taxa characteristic of diet intervention, including *Bifidobacterium* bloom in HFRS (**E**). The LDA of 4.0 was used for the GALAXY cladogram. Data are presented as the mean ± SEM; $^{a, b, c}$ different letters indicate statically significant ($p < 0.05$) differences among groups. HF = high fat, HFRS = high-fat resistant starch, $n = 8$ per group.

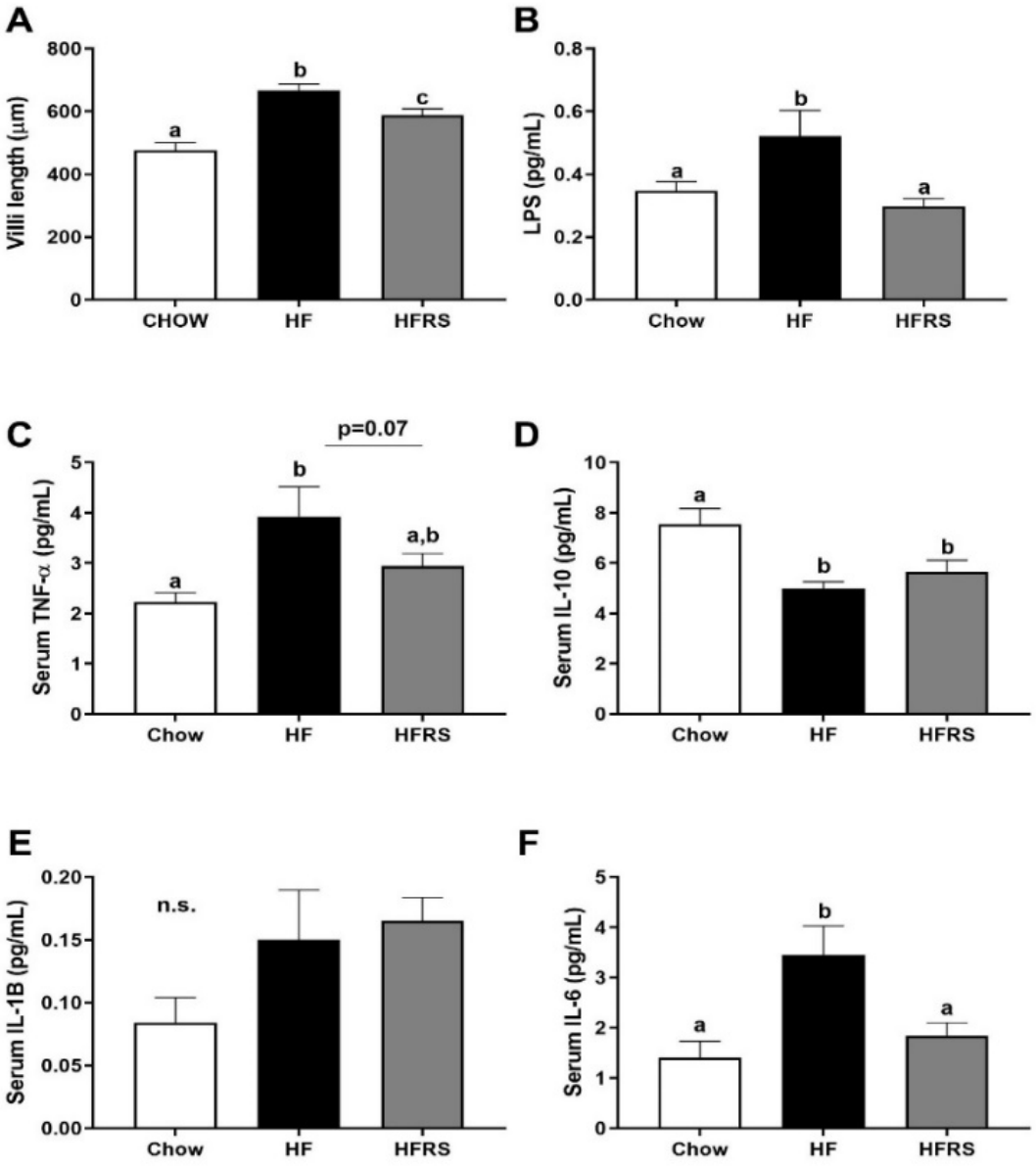

Figure 2.3. Potato RS attenuates GI hypertrophy and systemic inflammation. The HF diet increased villi length compared to chow control which were reduced in RS supplemented rats (**A**). The HF feeding led to a significant increase in pro-inflammatory LPS circulating levels, which was normalized by RS supplementation (**B**). Similarly, HF-diet driven increases in circulating TNFα (**C**) and IL-6 (**F**) were reduced in HFRS rats. Both HF and HFRS animals display a significant decrease in circulating IL-10 (**D**). There were no differences among groups in serum IL-1β (**E**). LPS = lipopolysaccharides, TNFα = tumor necrosis factor-a, IL-10 = interleukin 10, IL-6 = Interleukin 6, IL-1β = Interleukin 1 Beta, HF = high fat, HFRS = high-fat resistant starch, all significance determined at $p < 0.05$. $n = 8$ per group. Data are presented as the mean ± SEM; [a, b, c] different letters indicate statically significant differences among groups.

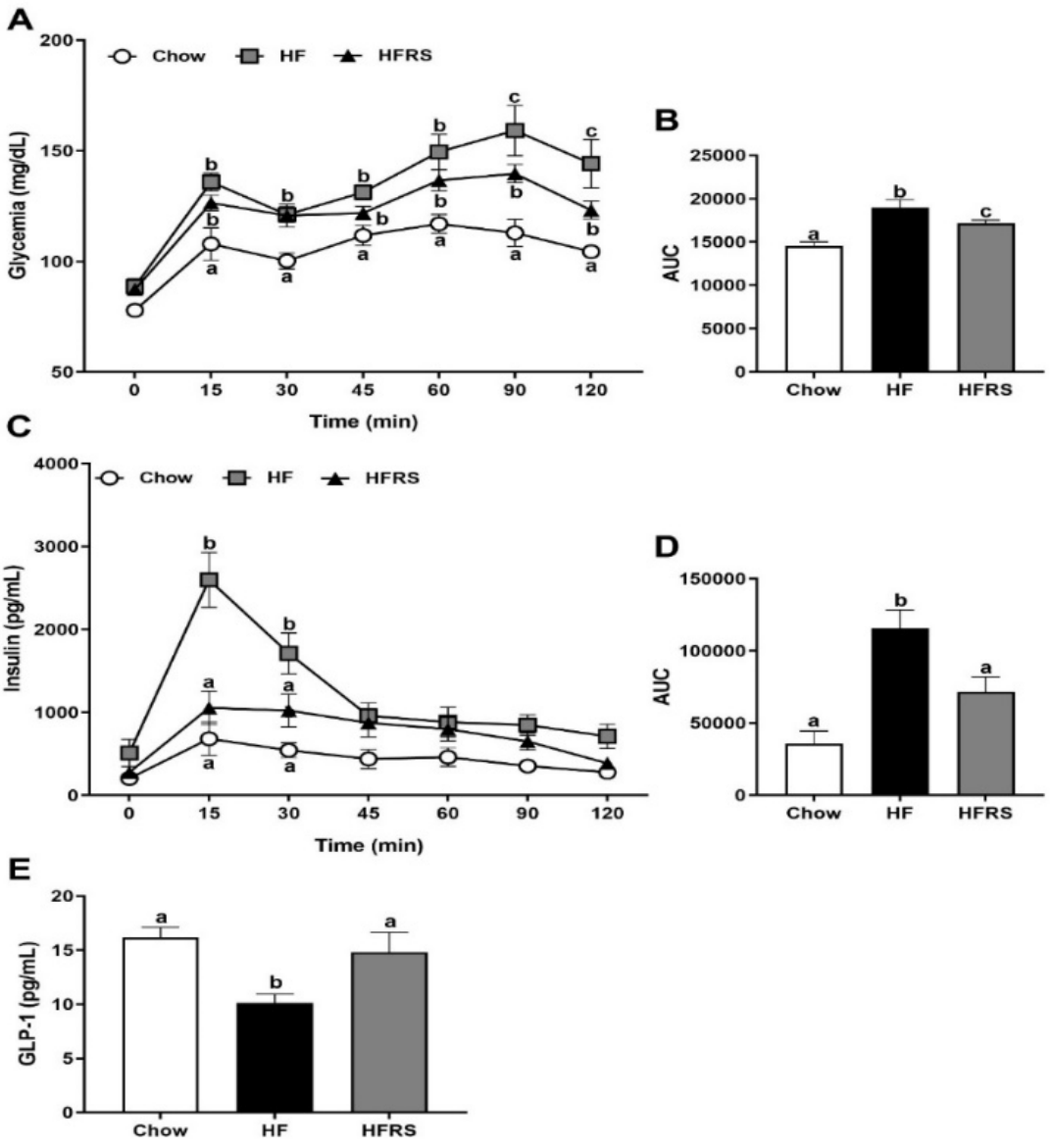

Figure 2.4. Potato RS improves glucose homeostasis. There was a significant increase in glycemia in all HF rats compared to chow animals in response to glucose, but HFRS rats recovered faster than HF; glycemia was significantly lower at 90 and 120 min in HFRS compared to HF (**A**). A significantly higher AUC was observed in HF than chow, which was partially improved in HFRS (**B**). Insulinemia was significantly higher in HF rats compared to both chow and HFRS animals at 15 and 30 minutes post-oral gavage (**C**,**D**). There was a significant decrease in circulating GLP-1 in HF-fed rats after 8 weeks on the diet compared to chow and HFRS rodents (**E**). OGTT = oral glucose tolerance test, AUC = area under the curve, HF = high fat, HFRS = high-fat resistant starch. Data are presented as the mean ± SEM; [a, b, c] different letters indicate statically significant ($p < 0.05$) differences among groups, $n = 8$ per group.

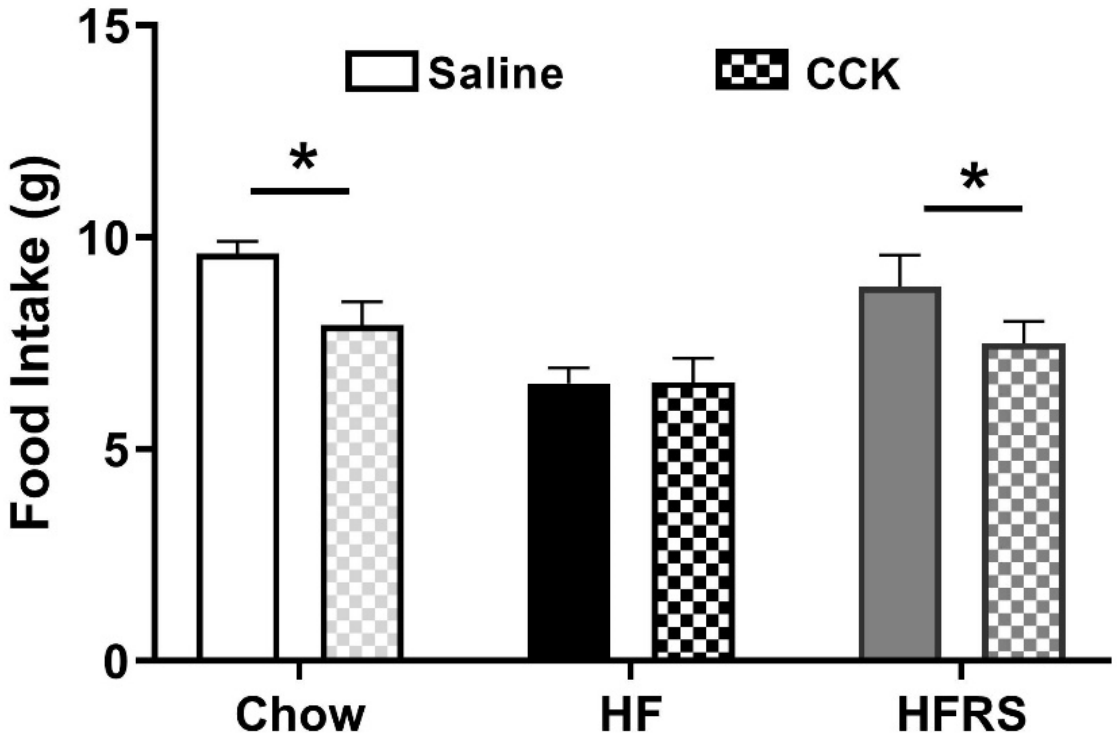

Figure 2.5. Potato RS prevents HF-driven loss in CCK sensitivity. Two hours post i.p. injection, chow and HFRS animals significantly decreased food intake when injected with CCK; compared to saline injection, HF rodents did not significantly decrease food intake with CCK injection. CCK = cholecystokinin, i.p., = intraperitoneal, HF = high fat, HFRS = high-fat resistant starch, * indicates significance determined as $p < 0.05$. $n = 7–8$ per group. Data are presented as the mean ± SEM.

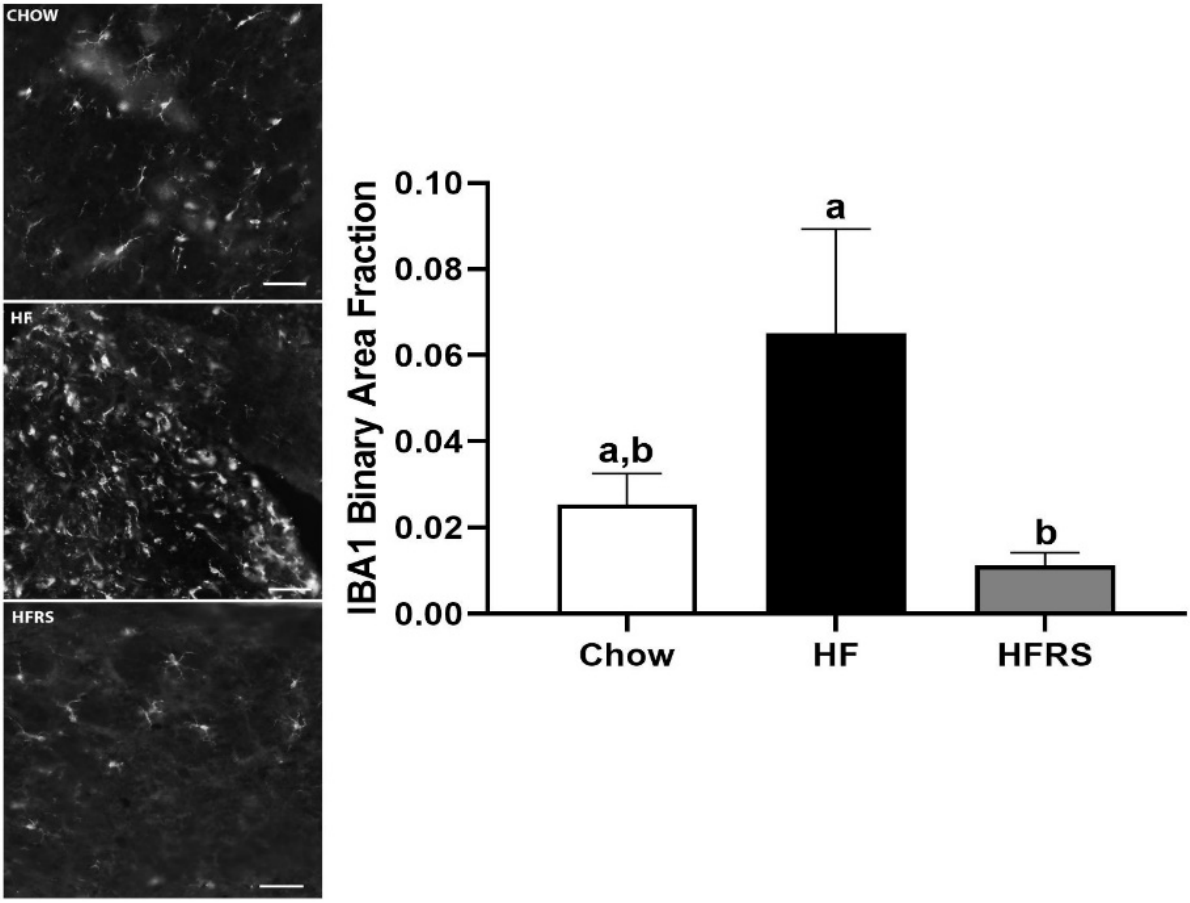

Figure 2.6. Potato RS prevents hindbrain inflammation. Fluorescent staining for IBA1 quantification showed a significant increase in positive staining in the NTS of HF-fed rats compared to HFRS animals (**right**). Representative images showing positive staining and morphology of microglia in chow, HF, and HFRS NTS sections (**left**). NTS = nucleus tractus solitarius, IBA1 = isolection B-alpha 1, HF = high fat, HFRS = high-fat resistant starch, [a, b, c] different letters indicate statically significant ($p < 0.05$) differences among groups, $n = 6–7$, scale bar = 50 μm.

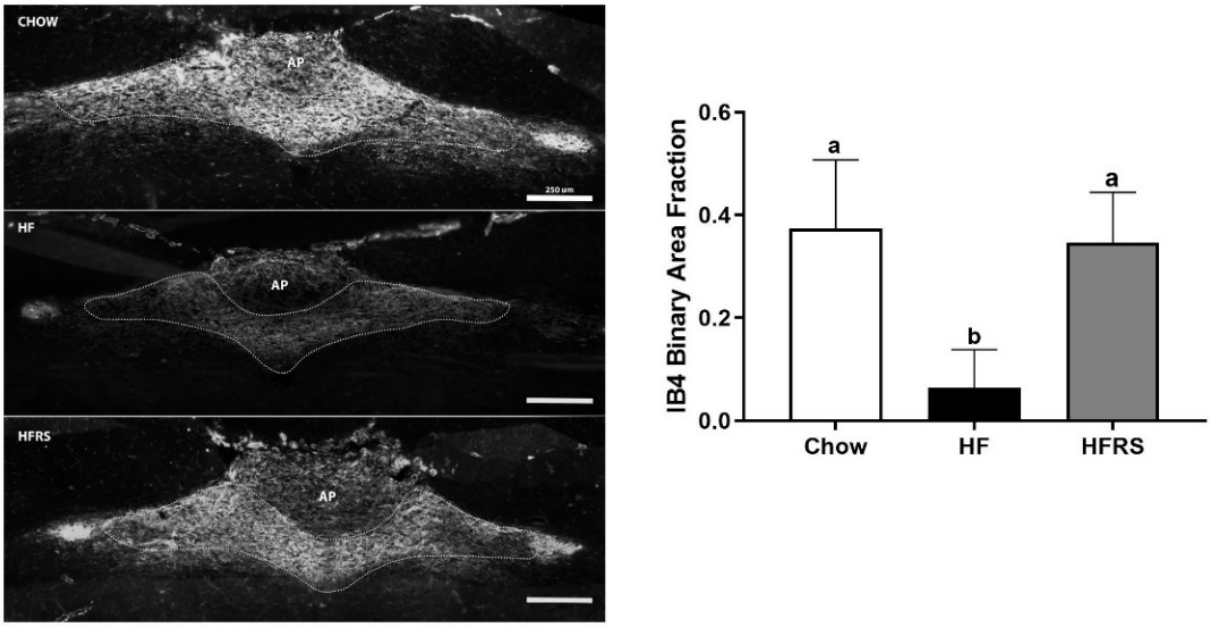

Figure 2.7. Potato RS prevented vagal remodeling. Representative NTS sections showing IB4 in chow, HF, and HFRS animals; the medial NTS at the level of the area postrema is outlined in white dashes (**right**), positive staining was quantified in the marked area (**left**). NTS = nucleus tractus solitarius, IB4 = isolectin B4, HF = high fat, HFRS = high-fat resistant starch. Data are presented as the mean ± SEM; [a, b, c] different letters indicate statically significant ($p < 0.05$) differences among groups, $n = 8$. Scale bar = 250 μm.

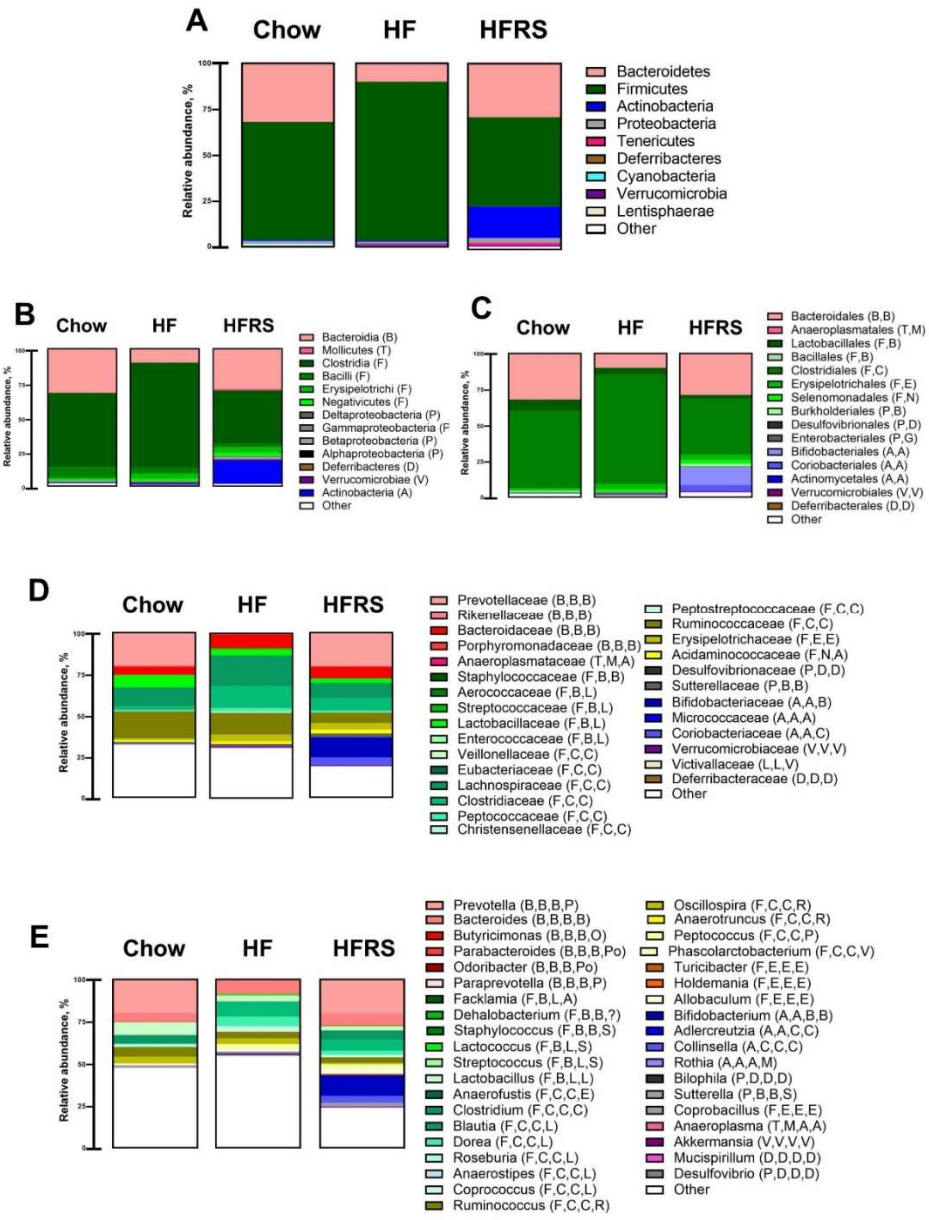

Supplemental Figure S2.1. Microbiota Abundance by Taxonomic Level: Microbiota abundances for Chow, HF, and HFRS. Phyla: B: *Bacteroidetes*, F: *Firmicutes*, T: *Tenericutes*, P: *Proteobacteria*, A: *Actinobacteria*,V: *Verrucomicrobia* Class: B: *Bacilli*, B: *Bacteroidia*, C: *Clostridia*, E: *Erysipelotrichia*; M: *Mollicutes*, N: *Negativicutes*, D: *Deferribacteres*, A: *Actinobacteria*, V: *Verrucomicrobiae*, B: *Betaproteobacteria*. Order: B: *Bacteroidales*, C: *Clostridiales*, L: *Lactobacillales*, E: *Erysipelotrichiales*, B: *Burkholderiales*, B: *Bifidobacteriales*. Family: C: *Clostridiaceae*, L: *Lachnospiraceae*, R: *Ruminococcaceae*, L: *Lactobacillaceae*, E: *Erysipelotrichaceae*, D: *Desulfovibrionaceae*, B: *Bifidobacteriaceae*, V: *Verrucomicrobiaceae*, A: *Acidaminococcaceae*. Phyla level (A), Class (B), Order (C), Family (D), and Genera (E). HF=high fat, HFRS=high fat resistant starch, n=8.

CHAPTER 3

MANIPULATION OF FEEDING PATTERNS MODULATES MICROBIOTA COMPOSITION, IMPROVES INFLAMMATORY TONE AND GLUCOSE TOLERANCE, AND MAINTAINS VAGALLY-MEDIATED SATIETY SIGNALING[3]

[3] Adapted from Klingbeil EA, Schade R, Lee SH, Kirkland R, de La Serre CB. Manipulation of feeding patterns modulates microbiota composition, improves inflammatory tone and glucose tolerance, and maintains vagally-mediated satiety signaling. To be submitted to: American Journal of Physiology-Regulatory, Integrative and Comparative Physiology.

Abstract

Background: Consumption of high fat diets (HF) have been shown to increase meal size and meal frequency resulting in overeating. Reducing meal frequency and establishing periods of fasting, independently of caloric intake, may improve obesity-associated metabolic disorders. Evidence suggests that gut microbiota HF alteration in gut microbiota play a role in diet induced obesity and metabolic disorders.

Objective: In this study, we hypothesized that manipulation of feeding patterns via time restricted feeding would improve microbiota composition.

Methods: Male Wistar rats were placed in three groups with each group consuming a HF, low fat diet (LF), or pair-fed HF diet for 7 weeks (n=4-8/group). Pair-fed animals received the same amount of food consumed by the HF fed group once daily before their dark cycle (HF-PF). Rats underwent an oral glucose tolerance and cholecystokinin sensitivity tests. Bacterial DNA was extracted from the cecum and feces collected during both dark and light cycles and sequenced via Illumina MiSeq sequencing of the 16S V4 region.

Results: Our pair-feeding paradigm reduced meal numbers without changing total caloric intake. Data analyses revealed a consistently lower *Firmicutes:Bacteriodetes* ratio in HF-PF animals compared to the HF rats, and HF-PF animals had restored cyclical bacterial abundances lost in HF feeding. Additionally, HF-PF rats had improved inflammatory status, glucose homeostasis and restored CCK-induced satiety compared to the HF group.

Conclusion: Time restricted feeding led to composition changes in gut microbiota that resulted in metabolic improvements via glucose homeostasis and CCK-induced satiety signaling.

Key words: Time restricted feeding, gut microbiota, glucose homeostasis, satiety signaling, vagus nerve

Introduction

Between 1980 and 2013, the prevalence of overweight and obesity in the U.S. increased from 56.7% to 70.9% in men and from 43.9% to 61.9% in women [71]. Consuming diets high in calorie-dense foods, such as high-fat diets (HF), promotes the development of hyperphagia [4]. Hyperphagia results in weight gain by increasing feeding frequency and consumption of foods at irregular times [72]. The changes in glucose levels caused by feeding is a major aspect of peripheral circadian regulation. Normal feeding patterns involve structured meals, resulting in glucose levels rising and falling at certain levels throughout the day, with a major increase in the morning when the first meal is consumed and a decrease at night during rest [73]. National Health and Nutrition Examination Surveys (NHANES) indicate that over time, Americans have been increasing their caloric intake, and snacks (defined as food ingested between meals) account for approximately 20% of calories consumed daily [74]. Thus, 20% of calories are being consumed apart from structured meals, implying that glucose levels lose a certain degree of circadian rhythmicity. In rodents, HF has been shown to promote hyperphagia, resulting in locomotor and feeding activity during light phases when these animals would normally be at rest [75]. This behavior mirrors nighttime snacking behaviors in humans and the results of the 2010 NHANES survey, which suggests that 8% of daily calories are consumed as snacks after dinner [74]. Loss of rhythmicity in glucose levels adversely impacts circadian regulation in the gastrointestinal (GI) tract, which can result in loss of rhythmicity in secretion of hormones necessary for metabolism and feeding regulation [76]. Furthermore, increased frequency of food entering the GI tract impacts microbiota composition, which also fluctuates in a circadian pattern due to abundances of certain microbes increasing and decreasing in response to feeding [77].

The gut microbiota consists of more than 10^{14} bacteria [8]. The two major phyla present in the GI tract are *Firmicutes* and *Bacteriodetes* [8]. An increased ratio of *Firmicutes:Bacteriodetes* has been associated with obesity and obesity-related pathologies such as pre-diabetes or insulin resistance [78]. The low-grade inflammation characterized in obesity is caused, at least partially, by the gut microbiota [11]. A "leaky gut" allows pro-inflammatory factors, such as lipopolysaccharides (LPS), produced by gut bacteria into circulation, promoting systemic inflammation [11]. Constant administration of low doses of LPS results in systemic inflammation and insulin resistance in rodents [11]. There is also evidence to support that chronic, low-grade inflammation may adversely impact vagal signaling through loss of c fibers in the Nucleus Tractus Solitarius (NTS), located in the hindbrain [79]. The vagal nerve has receptors for hunger and satiety hormones secreted in the GI tract and, thus, is a central component of gut-brain signaling for feeding regulation. Cholecystokinin (CCK), a potent satiety hormone released by I cells in the ileum in response to the presence of lipids and proteins, binds to CCKR1 on the vagus, inhibiting hunger signals to the NTS while satiety signals are promoted [79]. If vagal signaling is compromised, CCK released in response to feeding is unable to signal satiety to the NTS and promote meal termination. In standard fed rodents, *Firmicutes* abundance peaks during dark, or active feeding, cycles while *Bacteriodetes* abundance peaks during fasting, or light, periods [80]. This cycle is lost with HF feeding in animals, with *Firmicutes* dominating at all times [77]. Because an imbalance of *Firmicutes* is associated with low-grade, systemic inflammation, dysbiosis resulting from HF consumption likely contributes to impaired vagal signaling. This is supported by time-restricted feeding experiments in which rodents only had access to HF food for certain periods of time. Forced maintenance of circadian feeding patterns maintains cyclic fluctuations in microbiota composition [77] and circulating glucose levels, and

these animals have lower adiposity and better glucose tolerance than their *ad libitum*-fed counterparts [81]. These studies demonstrate the importance of considering meal frequency in addition to energy intake when addressing metabolic issues. Our study uses a time-restricted feeding paradigm to determine the effects of meal frequency on microbiota composition, fat mass, gut health, insulin resistance and satiety signaling in the presence of HF. The data from this study are necessary to understand how maintaining circadian fluctuations in microbiota composition alleviates the impacts of HF on glucose homeostasis and gut-brain signaling.

Methods

Experiment 1: Male Wistar rats (Envigo, Indianapolis, IN, USA) were placed in three groups with each group consuming a low fat (LF, 10% fat, D12450H, Research Diets, New Brunswick, NJ, USA, n=8) or HF diet (45% fat, D12451, Research Diets, n=15) for 7 weeks (Supplemental Table 1). A subset of HF fed animals (HF pair-fed, HF-PF, n=7) received their daily caloric intake once a day. The caloric amount matched that consumed by the *ad libitum* HF group. Animals were singly housed and body weight and food intake was recorded daily.

Insulin Tolerance Test: At during week 6, animals were fasted for 5 hours before initial blood collection via tail nick. Immediately following baseline collection, rodents were injected with insulin (1000 mU/kg, Sigma-Aldrich, St. Louis, MO, USA) and blood was sampled for glycemia using a glucose monitor (Freestyle, TheraSense, Alameda, CA, USA) at 15, 30, 45, 60, 75, 90, 105 and 120 minutes post-injection.

CCK Sensitivity Test: At 6 weeks, animals were fasted for 12 hours before receiving intraperitoneal injections of CCK (Bachem, Torrance, CA, USA) at a dose of 0.22 nmol/kg or vehicle of saline at 400 ul. Intake was measured 2 hours post injection.

16S rRNA Extraction and Sequencing: Cecal samples were collected during sacrifice. Bacterial DNA was extracted with a commercial kit (Zymo Research, Irvine, CA, USA) and sent to the SeqMatic facility (Fremont, CA, USA) for sequencing. The V3-V4 regions of the16s rRNA gene was amplified and targeted for sequencing by Ilumina MiSeq (Illumina, San Diego, CA, USA). These sequences were demultiplexed and assigned to organizational taxonomic units (OTUs) by QIIME [82]. These OTUs were then assigned to taxa by the Greengenes [83] database through the QIIME pipeline.

*Experiment 2: Meal Patterning***:** Male Wistar rats (Envigo, Indianapolis, IN, USA) were placed in three groups with each group consuming either a LF (10% fat, D12450H, Research Diets, n=4) or HF diet (45% fat, D12451, Research Diets, n=8) for 7 weeks **(Supplemental Table S3.1)**. A subset of HF fed animals (HF-PF, n=4) received their daily caloric intake once per day before the onset of the dark cycle. The caloric amount matched that consumed by the *ad libitum* HF group. Animals were singly housed in feeding pattern cages containing Biodaq (Research Diets) devices that recorded the time points at which food was consumed and the amount of food consumed at each of these feeding bouts. Meals were defined based on the intervals between feeding bouts. When these intervals exceeded 30 minutes, the bout following the 30-minute feeding break was defined as the beginning of a new meal. Recorded food intake in grams was used to calculate caloric intake.

Body Weight/Composition and Tissue Collection: Body weight was measured daily, and body composition was determined using a Minispec LF 110 BCA Analyzer (Bruker Crop., The Woodlands, TX, USA). Immediately following sacrifice at the onset of the dark cycle, ileum, colon, liver, and brain tissues were harvested and flash frozen on dry ice. Samples were then stored at -80 C until analyses.

Liver Oil Red O: Livers were cryosectioned at approximately 8 um (Leica CM1900, Leica Biosystems, Wetzlar, Germany) and then sent for Oil red O staining at the histology laboratory of the University of Georgia. Photos of sections were taken at 40x on a Nikon ECLIPSE TS100-F (Nikon, Tokyo, Japan) inverted microscope within 24 hours of stain completion. Images were analyzed for red pixel density using Scion Image (Frederick, Maryland, USA). Lower index was averaged for all images before analysis. Pixel count was then transferred to an excel spreadsheet for final analysis.

Gut Tissue: Ileum and colon samples were cryosectioned at approximately 4 um (Leica Biosystems) then post-fixed using 10% paraformaldehyde before staining. *Goblet Cell Quantification and Villus Measurement*: Ileum slides were incubated in acetic acid for 3 minutes, followed by a 30-minute incubation in Alcian Blue (pH 2.5, abcam, Cambridge, MA, USA) at room temperature. Slides were then rinsed and stained in Nuclear Fast Red (Sigma-Aldrich, St. Louis, MO, USA) for 5 minutes. Slides were washed again with DI water and dehydrated by incubating 1 minute in 95% ethanol, followed by three quick changes in 100% ethanol and Citrisolv (Decon Labs, King of Prussia, PA, USA). Slides were then mounted with Cytoseal 60 (Thermo Fisher Scientific, Waltham, MA, USA) and dried before imaging. Alcian blue stained sections were imaged using a Nikon ECLIPSE TS100-F (Nikon) inverted microscope at 40x. Goblet cells were counted per crypt and recorded. Villi were imaged at 20x. Villus height was measured using Nikon Imaging (Nikon) software from the base of villi to the tip. Measurements were then complied in an excel spreadsheet for each image.

16S rRNA Extraction and Sequencing: Fecal samples were collected during dark and light periods each week. Bacterial DNA was extracted with a commercial kit (Zymo Research, Irvine, CA, USA) and sent to the SeqMatic facility (Fremont, CA, USA) for sequencing. The

V3-V4 regions of the16s rRNA gene was amplified and targeted for sequencing by Ilumina MiSeq (Illumina, San Diego, CA, USA). These sequences were demultiplexed and assigned to organizational taxonomic units (OTUs) by QIIME [82]. These OTUs were then assigned to taxa by the Greengenes [83] database through the QIIME pipeline.

Real-time PCR: mRNA was extracted from ileum and mesenteric fat samples using the RNeasy Mini Kit (Qiagen, Valencia, CA). cDNA was synthesized using the RevertAid First Strand cDNA Synthesis Kit (Thermo Fisher Scientific, Franklin, MA). RT-PCR was run on a StepOnePlus real-time PCR system (Thermo Fisher Scientific) using SYBR Green PCR master mix (Thermo Fisher Scientific) and IL-1B, IL-10, CD68, MCP-1, DefB2, REG3r primers purchased from Integrated DNA Technologies **(Supplemental Table S3.2).** Data were analyzed according to the $2^{-\Delta\Delta Ct}$ method [84].

C Fiber Quantification: Hindbrains were cryosectioned at 20 um (Leica Biosystems) from the caudal through the rostral region, at the level of the NTS. These sections were stained for isolectin B4 (IB4, Novuz Biologicals, Littleton, CO, USA), which stains unmyelinated vagal afferent c fibers.

Immunofluorescence: Sections were fixed in 4% paraformaldehyde for 15 minutes followed by 3x10 minute PBS washes. Blocked with 10% goat serum, sections were incubated with primary antibody IB4 (Novus Biologicals), washed, and incubated in the secondary ExtrAvidin—Cy3 (Sigma-Aldrich). Sections were mounted with fluoro gel (Electron Microscopy Sciences, Hartfield, PA, USA). Images of the NTS were captured at 20x magnification via a Nikon 80i imaging photomicroscope (Nikon) and stitched with a Nikon Digital Sight DS-Qi1Mc digital camera (Nikkon) as previously described [6]. IB4 fluorescence was quantified at the level of the Area Postrema under the same methods using binary imaging

using the Nikon Elements AR 3.0 Imaging software (Nikon) based on principles described in [85].

CCK Sensitivity Test: At 6 weeks, animals were fasted for 12 hours before receiving intraperitoneal injections of CCK (Bachem) at a dose of 0.22 nmol/kg or vehicle of saline at 400 ul. Intake was then measured 2 hours post injection.

Oral Glucose Tolerance Test: An oral glucose tolerance test (OGTT) was performed after 6 weeks on respective diets. Animals received a dose of glucose (2g/kg) via oral gavage. Glucose levels in blood collected from the tail were recorded at baseline, and 20, 40, 60, 80, and 120 minutes following an oral glucose challenge using a glucometer (Freestyle, Alameda, CA, USA). Insulin levels were measured from the blood samples collected at each of these time points using an insulin enzyme-linked immunosorbent assay (ELISA, Alpco, Salem, NH, USA).

Statistics: Data from gut tissue, liver oil red o, and the CCK challenge were analyzed using GraphPad Prism (Prism 7; GraphPad Software, La Jolla, CA, USA). One-way ANOVA was used to determine significant group differences. *Microbiota Analysis*: The METAGENassist[86] platform was used to filter out taxa with greater than 75% zero abundances in the OTU table, and unassigned and unmapped reads were also excluded during filtering. A generalized log transformation was used to normalize the data by taxon, and relative abundances were also determined for the filtered data. Taxa with significantly different abundances were detected by performing one-way ANOVAs on the normalized data at each taxonomic level. Pearson's r and Ward's clustering were used to construct dendrograms based on correlations between samples and taxa, and principal component analysis (PCA) was performed at each taxonomic level. The Galaxy platform was used to perform multivariate analysis using the linear discriminant analysis effect size (LEfSe) to identify taxonomic features discriminating of one or

more groups. *OGTT Analysis:* GraphPad Prism was used to analyze glycemia and Insulinemia data from the OGTT. Glycemia was compared among time points and diet groups via 2-way ANOVA with multiple comparisons by uncorrected Fisher's LSD. AUC for glycemia was determined for each animal and compared among groups via one-way ANOVA. Insulinemia was compared among time points and diet groups via 2-way ANOVA with multiple comparisons by uncorrected Fisher's LSD. AUC for insulinemia was determined for each animal and compared among groups via one-way ANOVA.

Results

Cohort 1: There were no significant differences in weight between groups (LF 459.8±14.6 vs HF 478.0±10.8 vs HF-PF 481.5±7.2 g at sacrifice, $p>0.05$) **(Figure 3.1A)**. HF diet significantly increased energy intake compared to LF (LF 78.5±4.3 vs HF 90.0±3.1 vs HF-PF 90.2±1.2 kcal, $p<0.05$) **(Figure 3.1B)**. HF rodents had decreased insulin sensitivity compared to LF controls during an insulin tolerance test (LF 75.5±6.0 vs HF 72.0±6.4 mg glucose/dL, $p<0.05$) while pair-feeding restored insulin sensitivity (HF 72.0±6.4 vs HF-PF 56.0±4.4 mg glucose/dL, $p<0.05$) **(Figure 3.1C)**. Interestingly, during LF and HF rodents were not sensitive to a low dose of intraperitoneal CCK (LF saline 19.2±1.7 vs LF CCK 18.3±1.5 kcal, $p>0.05$; HF saline 30.2±2.1 vs HF CCK 27.0±2.7 kcal, $p>0.05$), while pair-feeding restored CCK sensitivity (HF-PF saline 28.8±4.6 vs HF-PF CCK 20.1±3.8 kcal, $p<0.05$) **(Figure 3.1D)**. Other data from this study have been published previously [87].

Cohort 2: Feeding Patterns and Body Composition: There were no significant differences in total body weight **(Fig. 3.2A)** or lean body mass percentage between groups, while LF animals had significantly lower percentages of fat mass than HF (LF 29.7±0.3 vs HF 36.2±1.3 %fat mass, $p<0.05$, or HF-PF 36.0±1.2 %fat mass, $p<0.05$) or HF-PF animals **(Fig.**

3.2B). Average daily energy intake was significantly lower in LF animals (LF 84.5±1.6 vs HF 100.8±3.3 kcal, $p<0.05$; LF vs HF-PF 102.1±2.5 kcal, $p<0.05$) and did not significantly differ between the HF and HF-PF (HF 100.8±3.3 vs HF-PF 102.1±2.5 kcal, $p<0.05$) groups **(Fig. 3.2C)** at week 1 and this continued throughout the entirety of the study. HF feeding did not increase energy intake during the dark cycle compared to LF but did increase energy intake during the light cycle (week 7: LF 7.8±2.9 vs HF 16.6±2.4 kcal, $p<0.05$) **(Figure 3.2D)**. Pair-feeding significantly increased energy intake during the dark cycle (week 7: HF 67.1±7.0 vs HF-PF 76.6±1.3, $p<0.05$) and significantly decreased energy intake during the light cycle (week 7: LF 7.8±2.9 vs HF-PF 0.0±0.0 kcal, $p<0.05$) **(Figure 3.2D)**. HF rodents did not increase average meal size compared to LF controls in dark or light cycles **(Figure 3.2E)** while HF-PF rodent had significantly increased meal sizes during the dark cycle (week 7: LF 13.1±0.5 vs HF-PF 22.5±1.5 kcal, $p<0.05$) and decreased meal size during the light cycle (week 7: LF 6.6±1.3 vs HF-PF 0.0±0.0 kcal, $p<0.05$) **(Figure 3.2E)**. Consequently, HF rodents saw an increase in number of meals during the dark and light cycles (dark LF 5.5±0.4 vs HF 6.8±0.5 meals, $p<0.05$; light LF 0.8±0.1 vs HF 1.7±0.2 meals, $p<0.05$) **(Figure 3.2F).** Pair-feeding did not impact meal number during the dark cycle, but significantly decreased the number of meals during the light cycle (HF 1.7±0.2 vs HF-PF 0.2±0.1 meals, $p<0.05$) **(Figure 3.2F)**. Overall, HF feeding increased the number of small meals during the light, inactive cycle. Based on the meal size distribution, HF-PF animals consumed fewer, larger meals during the dark cycle and limited energy intake during the light cycle **(Figure 3.2G)**.

Tissue Analyses: LF animals had significantly lower fat levels in liver sections than HF-PF animals (LF 100.0±1.8 vs HF-PF 113.5±3.3 %, $p<0.05$), as indicated by pixel counts from oil red O staining **(Fig. 3.3A)**, while there was no significant difference between the HF and HF-PF

animals (HF 105.3±2.4 vs HF-PF 113.5±3.3 %, $p>0.05$). Gastrointestinal health was assessed in terms of villi heights and goblet cell counts. Villi height was significantly different in all three diet groups **(Fig. 3.3B)**, with LF having the tallest villi followed by HF-PF (LF 780.8±8.6 vs HF-PF 591.5±5.8 um, $p<0.05$) and HF (HF 484.4±36.6 vs HF-PF 591.5±5.8 um, $p<0.05$), respectively. Goblet cell counts were significantly different in all three groups as well **(Fig. 3.3C)**. HF averaged the highest number of goblet cells/crypt (LF 11.8±0.2 vs HF 12.9±0.1 cells/crypt, $p<0.05$), while HF-PF animals averaged the lowest (LF 11.8±0.2 vs HF-PF 9.4±0.1 cells/crypt, $p<0.05$).

Microbiota Composition: Partial Least Square Discriminant Analysis (PLS-DA) along with abundances and cladogram **(Fig. 3.4A,C-D)** show that pair-feeding resulted in a microbiota profile different than HF animals. Both cohorts saw an increase in *Ruminococcus, Lachnospiraceae, and Phascolarctobacterium* in response to HF diet while pair feeding significantly decreased abundance of these bacteria **(Fig. 3.4B)**. By week 5, the HF group demonstrated a dysbiotic microbiota profile no longer undergoing cyclical changes **(Fig. 3.5).** Interestingly, the HF-PF group demonstrated different trends in *Firmicutes*:*Bacteroidetes* ratio patterns during light and dark cycles relative to the LF and HF groups **(Fig. 3.5A-B).** While the differences were not significant, during dark cycles, HF-PF tended to have the highest *Firmicutes:Bacteroidetes* ratios, and during light cycles it had the lowest *Firmicutes:Bacteroidetes* ratios (**Fig. 3.5B**). *Clostridium* and *Lactobacillus* abundances did not differ between light and dark cycles in HF animals, while *Clostridium* significantly increased and *Lactobacillus* significantly decreased during the light cycle for HF-PF animals (**Fig. 3.5C-D).**

Oral Glucose Tolerance and Inflammation: The oral glucose tolerance test indicated significant differences in glucose homeostasis among groups. The HF group had significantly

higher glycemia levels at 60 and 80 minutes relative to the LF (60 min LF 105±11.2 vs HF 153±8.9 mg/dL, $p<0.05$; 80 min LF 116±9.1 vs HF 153±5.5 mg/dL, $p<0.05$) and HF-PF (60 min HF-PF 130±4.8 vs HF 153±8.9 mg/dL, $p<0.05$; 80 min HF-PF 130±9.6 vs HF153±5.5 mg/dL, $p<0.05$) groups after an oral glucose challenge, while glycemia was not significantly different between the LF and HF-PF groups **(Fig. 3.6A)**. Interestingly, the HF-PF group had significantly higher insulin levels relative to the LF and HF groups up to 40 minutes following the oral glucose challenge (20 min LF 5.3±1.0 vs HF-PF 7.1±0.5 mg/dL, $p<0.05$ and HF-PF 7.1±0.5 vs HF 4.0±0.8 mg/dL, $p<0.05$; 40 min LF 3.0±1.1 vs HF-PF 5.0±0.7 mg/dL, $p<0.05$ and HF-PF 5.0±0.7 vs HF 3.1±0.7 mg/dL, $p<0.05$), after which insulin did not significantly differ among groups **(Fig. 3.6B)**. Real-time PCR on ileum cDNA found that HF animals had significantly increased expression of IL-1B (LF 1.0±0.5 vs HF 1.8±0.5 fold change, $p<0.05$), IL-10 (LF 1.0±0.4 vs HF 2.9±0.8 fold change, $p<0.05$), CD86 (LF 1.0±0.1 vs HF 2.5±0.4 fold change, $p<0.05$), MCP-1 (LF 1.0±0.1 vs HF 2.6±0.3 fold change, $p<0.05$) and Defb2 (LF 1.0±0.2 vs HF 3.7±0.7 fold change, $p<0.05$) compared to the LF control **(Fig. 3.6C)**. Interestingly, ileal expression of IL-1B, IL-10, CD68 and MCP-1 were not signifcantly different between LF and HF-PF groups. Defb2 gene expression was increased in HF-PF animals (LF 1.0±0.2 vs HF-PF 4.1±1.6 fold change, $p<0.05$) compared to LF and Reg3γ expression was significantly increased compared to both LF (LF 1.0±0.2 vs HF-PF 4.2±0.4 fold change, $p<0.05$) and HF (HF 0.6±0.2 vs HF-PF 4.2±0.4 fold change, $p<0.05$) animals. Mesenteric fat gene expression of IL-10 (LF 1.0±0.1 vs HF 2.1±0.6 fold change, $p<0.05$), CD68 (LF 1.0±0.3 vs HF 1.7±0.2 fold change, $p<0.05$) and MCP-1 (LF 1.0±0.3 vs HF 3.4±0.6 fold change, $p<0.05$) was significantly increased in HF animals compared to LF control **(Fig. 3.6D)**. Interestingly, HF-PF animals did not have significantly increased gene expressions of IL-10 and CD68 compared to LF controls, but did

have an increased expression of MCP-1 (LF 1.0±0.3 vs HF-PF 2.5±0.5 fold change, $p<0.05$). While HF-PF animals had significantly lower expressions of IL-10 (HF 2.1±0.6 vs HF-PF 0.9±0.3 fold change, $p<0.05$) and CD68 (HF 1.7±0.2 vs HF-PF 1.2±0.1 fold change, $p<0.05$) in mesenteric fat than HF animals, they were not significantly different in MCP-1 gene expression (HF 3.4±0.6 vs HF-PF 2.5±0.5 fold change, $p>0.05$).

Vagal remodeling and CCK sensitivity: HF-PF animals had significantly higher levels of IB4 binary area fraction in the NTS at the level of the area postrema than HF animals (HF 0.10±0.02 vs HF-PF 0.2±0.04 binary area fraction, $p<0.05$; **Fig. 3.7A**) but not LF animals (LF 0.14±0.02 vs HF-PF 0.2±0.04 binary area fraction, $p>0.05$). LF rodents did not decrease energy intake in response to CCK (LF saline 19.2±1.7 vs LF CCK 18.3±1.5 kcal, $p>0.05$) nor HF (HF saline 30.2±2.1 vs HF CCK 26.9±2.7 kcal, $p>0.05$). Interestingly, HF-PF animals significantly reduced energy intake in response to CCK (HF-PF saline 28.8±4.6 vs HF-PF CCK 20.1±3.8 kcal, $p<0.05$) **(Fig. 3.7B**).

Discussion

The first cohort investigated the impact of pair-feeding on body weight and found that pair-feeding did not change impact weight gain or energy intake. Interestingly, pair-feeding significantly changed glucose homeostasis and CCK sensitivity. Over the course of the second cohort, HF-PF and HF groups consumed the same number of calories, but the HF animals increased number of small meals during the inactive, light cycle, which is normally a fasting period. Previous research supports the finding that rodents fed a HF or cafeteria diet significantly increase the number of snacks, increasing overall energy intake and changing feeding patterns compared to chow controls [88, 89]. Meanwhile, the HF-PF group consumed significantly fewer meals, especially during light periods. This indicates that the pair-feeding paradigm successfully

modeled time-restricted feeding, and differences in metabolic profile and microbiota composition between these groups is due to temporal differences in feeding. Recently, researchers found that intermittent fasting improves behavioral impairment in diabetic mice [90] and these neuroprotective effects are partly abolished with the removal of the gut microbiota, supporting the significance of the bug-gut-brain axis in cognitive function. From this, we hypothesize that increased fasting periods may be driving cognitive changes via the gut microbiota composition, explaining the changes in feeding behavior we found in pair-fed animals.

Endpoint body weight did not significantly differ among groups, and at the end of the study, the two HF-fed groups did not differ in body composition, while LF animals had lower fat mass. These results reflect the isocaloric nature of the two HF diets and suggest that when the same amount of calories are consumed, changing the time at which these calories are consumed does change the impact on body weight. This was further demonstrated by the lack of significant differences in the liver fat content.

While pair-feeding did not impact body weight or adiposity, it did impact intestinal morphology. Pair-fed animals had significantly higher villi lengths relative to HF animals, thus causing them to have a phenotype between those of the LF and HF groups. Villus height undergoes circadian variation dependent on feeding status [91]. Therefore, since animals were sacrificed at the onset of the dark cycle, HF-PF rodents would be expected to have increased villi lengths due to fasting. Villi lengths also impact ability to absorb nutrients, and longer villi lengths are associated with healthy intestinal physiology [92] which has also been found with fiber supplementation [93]. Besides showing differences in villi lengths, the HF-PF group also had decreased goblet cell counts relative to HF animals. The primary function of goblet cells is

to secrete mucus, which maintains a barrier between intestinal cells and the microbiota [94] and chronic infection may result in a depletion of goblet cells, negatively impacting gut health [94].

Analysis of the gut microbiota supports the idea of the pair-fed group having a phenotype different than those of the LF and HF groups. By week 5, the impacts of diet on microbiota composition could be observed. Both cohorts experienced increases in several families of the order *Clostridiales* in response to HF diet. Both *Lachnospiraceae* and *Ruminococcus* have been to found to increase with high sugar diets [6]. *Ruminococcus* and *Phascolarctobacterium,* a genus of the order *Negativicutes,* increases in HF feeding [95, 96]. Least Discriminant Analysis identified the genus *Candidatus Arthromitus* as a unique characteristic of HF feeding in both cohorts. Recent research shows that *Candidatus Arthromitus* is positively correlated with triglycerides [96]. Importantly, pair-feeding consistently resulted in decreased abundances of these bacteria.

Despite consuming the same type and quantity of food as the HF group, animals in the HF-PF group demonstrated microbial abundance patterns intermediate to those of the LF and HF groups. Previous research shows that that these changes in microbiota rhythmicity influence metabolism [96]. While these shifts were not sufficient to produce significant changes at the global level, there are significant differences in levels of specific taxa, which cumulatively contribute to an intermediate microbiota phenotype. Furthermore, while differences in *Firmicutes*:*Bacteroidetes* ratios were not significant during dark or light cycles, there is a circadian trend in the HF-PF group in which these ratios appear higher during dark cycles, when these animals are feeding, and lower during light cycles, when these animals are fasting. An increased *Firmicutes*:*Bacteroidetes* ratio has been previously linked to negative health outcomes, resulting in dysbiosis [97]. Previous studies have found similar patterns in which

Firmicutes:Bacteroidetes ratios are higher during feeding and lower during fasting [77, 80], so this trend in the HF-PF group reflects the impact of time restricted feeding and enforced circadian feeding-fasting patterns. Both the LF and HF groups consumed more food during light cycles than the HF-PF group. This lack of circadian-based feeding patterns in the LF and HF groups may be reflected by constant *Firmicutes*:*Bacteroidetes* ratios across light and dark cycles. *Lactobacillus* significantly fluctuated between light:dark in HF-PF but not HF animals. Extensive research on *Lactobacillus* has indicated it impacts lipid accumulation [96] and oral administration improves insulin resistance and glucose intolerance [98]. The restoration of a cyclical microbiota composition in the HF-PF animals may be the reason for the maintenance of glucose homeostasis and satiety signaling in pair-fed rodents compared to HF. Time-restricted feeding of animals has previously been found to modulate microbiota composition and support gut integrity through the promotion of short-chain fatty acid-producing gut bacteria [99].

The LF and HF groups lacked the circadian fluctuations in *Firmicutes*:*Bacteroidetes* ratios seen in the HF-PF group, so *Firmicutes* abundances were chronically elevated in these animals. Recent evidence has shown that rhythmicity of *Firmicutes* is lost with HF feeding and restored with melatonin treatments [96]. *Firmicutes* is associated with inflammatory disorders involving translocation of LPS across the intestinal barrier [100]. Therefore, higher goblet cell counts in LF and HF animals may be part of a protective response in which mucus production increases in an effort to maintain gut barrier integrity in the presence of elevated *Firmicutes*. Interestingly, increased levels of REG3γ gene expression in HF-PF animals may be contributing to the maintenance of a more positive gut microbiota composition. An antimicrobial protein, REG3γ is produced by Paneth cells in the gut in the presence of commensal bacteria [101]. Notably, REG3γ is selectively bactericidal to Gram positive bacteria [102] and can bind

peptidoglycan, a pro-inflammatory molecule found on Gram positive bacteria [102]. With this in mind, upregulation of REG3γ may have been a mechanism to prevent HF diet-induced dysbiosis and metabolic disorders in pair-fed animals.

Increased gut function was associated with improved inflammatory status. LF and HF-PF animals had significantly lower levels of inflammation in the ileum and mesenteric fat tissue than HF rodents. Obesity has been associated with macrophage infiltration in adipose tissue [103] and gut leakiness is exacerbated via inflammation [104]. Previous findings in our lab have found HF diet-driven dysbiosis results in a decrease in short-chain fatty acid-producing bacteria and increase in serum inflammation [105]—which are important for gut integrity [106].

While glucose tolerance was best in the LF rats, which managed to maintain normal glycemia levels with a modest secretion of insulin in response to an oral glucose challenge, the HF-PF rats were able to maintain glycemia levels that did not significantly differ from those of the LF rats. The pronounced insulin response in the HF-PF rats may indicate that they may require more insulin than the LF rats in order to maintain the same glucose regulation, suggesting a certain degree of insulin resistance. Increased insulin resistance has been associated with microbiota dysbiosis and increased low-grade inflammation [105, 107] Alternatively, because the HF-PF rats have greater fluctuations in circulating glucose levels over 24-hour periods, they may be more sensitive to glucose than LF and HF rats, which constantly had elevated glucose due to snacking. Greater sensitivity to increases in circulating glucose levels could promote the robust insulin response seen in the HF-PF animals [108]. The HF rats do not secrete significantly different levels of insulin relative to the LF group and do not control glycemia as well as the HF-PF rats, so these rats appear to be insulin resistant and unable to compensate for this resistance.

Researchers have consistently found insulin resistance in relation to HF-diet and dysbiosis [5, 105, 109].

Dysbiosis is also associated with vagal remodeling [105] and microbiota manipulation has been shown to improve vagal remodeling and intake [6, 105]. HF-PF animals had significantly higher IB4 fluorescence in the area postrema than the HF group, but not the LF group, which indicates the presence of more unmyelinated c fibers and supports the idea that time-restricted feeding promotes the maintenance of unmyelinated c fibers in the NTS. Interestingly, the LF diet used in this study contains 17% sucrose, which has been found to decrease vagal afferent innervation at the level of the NTS and increase peripheral inflammation [6]. This could explain why LF rodents did not have a significantly higher amount of c fibers in the NTS. Because approximately 80% of c fibers in this region are from vagal afferents originating in the GI tract [110], it is likely that HF-PF animals may have more accurate food intake signaling between the gut and the brain. This finding is supported by the results of a CCK satiety signaling test in both cohorts. Food intake following CCK-injection decreased in pair-fed animals, but remained constant in LF and HF animals, indicating that time-restricted feeding was sufficient to maintain the CCK-induced satiation lost by HF or high-sugar feeding. CCK is secreted by I cells in response to the presence of lipids and proteins in the small intestine, and it signals satiety through the vagus nerve [79]. Consumption of HFD results in elevated plasma CCK levels, and previous studies have shown that HFD eventually results in decreased sensitivity to CCK and impaired satiation signaling [79].

Limitations and Perspective: Since we only had 12 Biodaq cages, we were limited to an n of 4 per group in the second cohort. Despite this limitation, we were able to replicate our findings in body weight, intake, microbiota composition, glucose homeostasis and CCK

sensitivity between both cohorts. Also, data from this study support the idea that changes in microbiota composition are sufficient to alter glucose homeostasis and CCK sensitivity. However, we are not able to determine based on the current data if such changes are necessary for the development of insulin resistance. Further research is necessary to provide evidence that microbiota changes are necessary for the progression on insulin resistance.

Conclusion

Notably, HF-PF rodents changed eating behaviors that positively impacted their metabolic outcomes despite HF diet. Time-restricted feeding, regardless of body weight, shifted microbiota composition towards that associated with a LF diet and restored circadian fluctuations in microbial abundances. HF-PF animals also maintained glucose tolerance due to robust insulin secretion in response to an oral glucose challenge. Lowered inflammatory status and CCK satiation sensitivity was also maintained in HF-PF animals, and this reflects the maintenance of gut-brain axis signaling. Time-restricted feeding maintained glucose homeostasis and vagally-mediated satiety signaling.

Supplemental Table S3.1. Macronutrient composition of LF, HF as a percent of energy[1]

Macronutrient	LF	HF
	% kcal	
Protein	18	18
Carbohydrate	71.3	35.7
Dextrose	2.5	2.5
Sucrose	18.4	18.4
Fructose	2.6	2.6
Fat	10.7	46.3
Total	100	100
	kcal/g diet	
	3.8	4.6

[1] Diets prepared by Research Diets, Inc. HF, high fat; LF, low fat.

Supplemental Table S3.2. Primer sequences used for qPCR[1]

Gene*	Forward primers (5' to 3')	Reverse primers (5' to 3')
Il-10	GGAAGTGGGTGCAGTTATT	GCTATGTTGCCTGCTCTT
Cd68	AAACAGTCCAGGCTTCTC	ATGGCTGGGAACCATTAG
Defb2	CGATGTCTAAGAGAGAAAGGG	GGAAACAGGTACCCACAAA
Gapdh	GAGCATCTCCCTCACAATTC	GGGTGCAGCGAACTTTAT
MCP-1	GGC TGG AGA ACT ACA AGA G	TCT GGA CCC ATT CCT TAT TG
Reg3r	CTT CCT TTG TGT CCT CCTT	CAC CTC TGT TGG GTT CTT
Il-1b	CATTGTGGCTGTGGAGAA	GCAGTGCAGCTGTCTAAT

[1]*Il-10,* interleukin-10; *Cd68*, cluster of differentiation 68; *Defb2***,** beta-defensin 2; *Gapdh,* glyceraldehyde 3-phosphate dehydrogenase; *MCP-1*, monocyte chemoattractant protein-1; *Reg3r*, regenerating islet-derived protein 3; *Il-1b*, interleukin-1 beta.

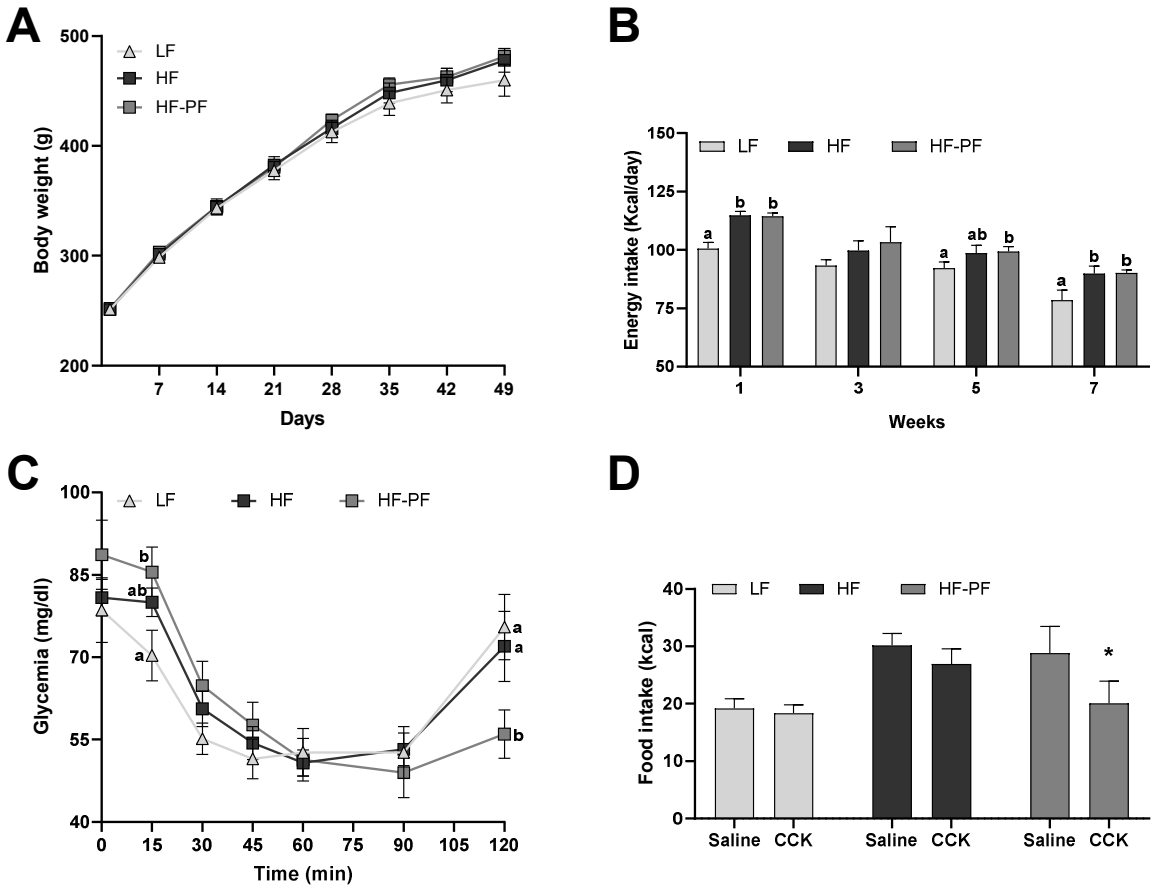

Figure 3.1. Pair-feeding changed the effects of HF diet. A) Body weight in grams throughout the 7 week experiment. B) Average calorie intake per group per week. C) Glycemia measured post oral glucose challenge during week 6. D) Food intake 2 hours post CCK or vehicle challenge during week 6. HF=high fat, HF-PF=high fat-pair-fed, CCK=cholecystokinin. n=7-8/group. Data presented as mean ± SEM; [a, b, c] different letters indicate statically significant ($p < 0.05$) differences among groups.

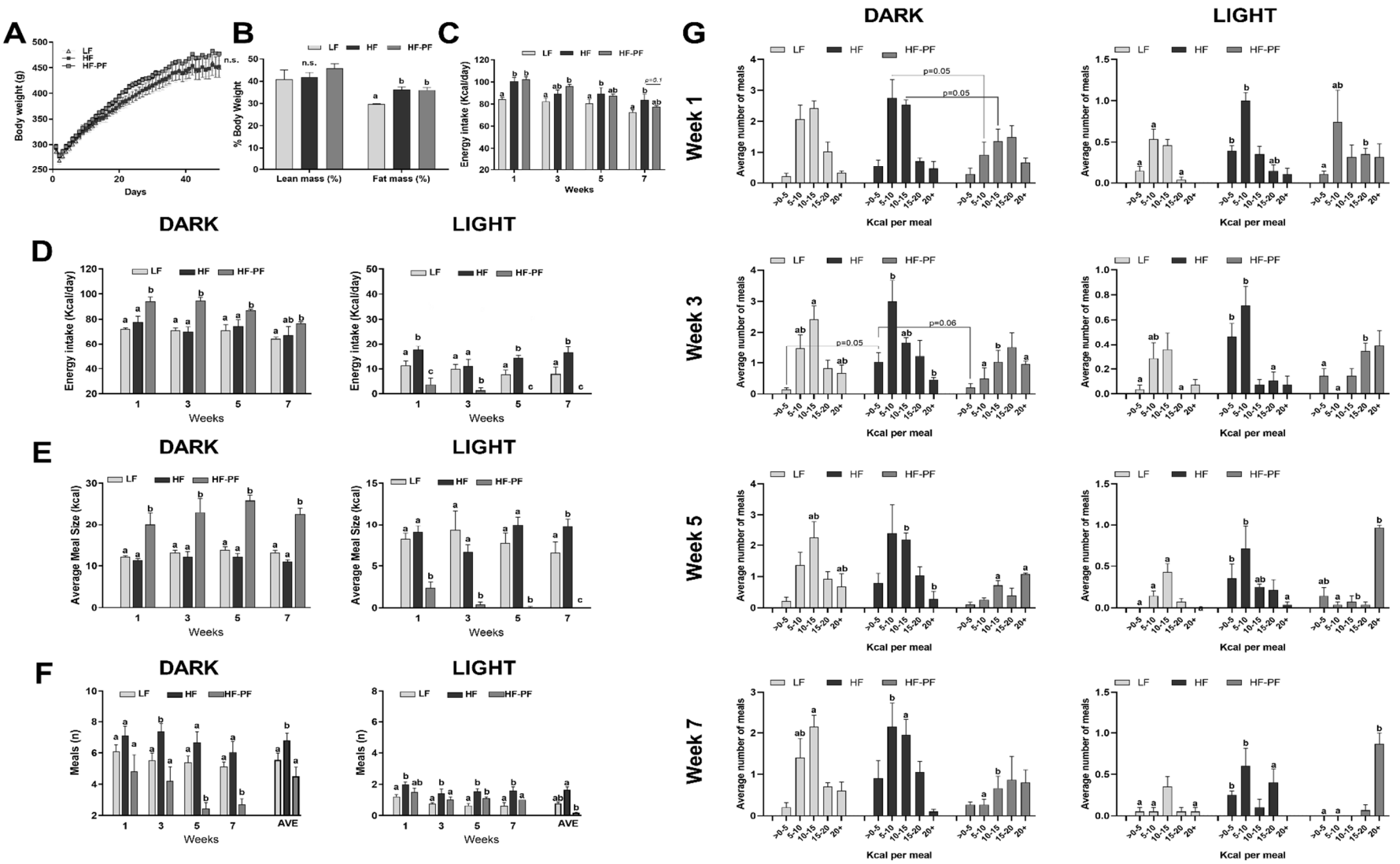

Figure 3.2. Pair-feeding impacted meal pattern but did not change kcal intake or body weight. A) Body weight in grams over experiment. B) Percent body weight in lean and fat mass. C) Average energy intake per group per week. D) Average energy intake per day per group during dark

and light cycles. E) Average meal size per group during dark and light cycles. F) Average meal number per day per group during dark and light cycles. G) Average meal size distribution during light and dark cycles. LF=low fat, HF=high fat, HF-PF=high fat-pair-fed. n=4/group. Data presented as mean ± SEM; [a, b, c] different letters indicate statically significant ($p < 0.05$) differences among groups.

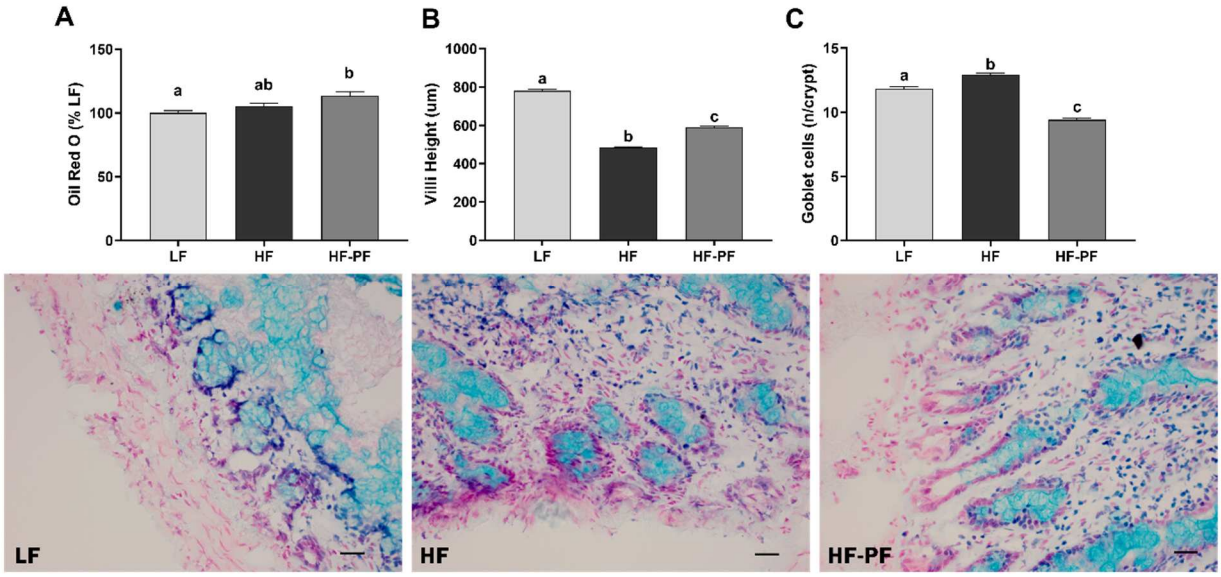

Figure 3.3. Pair-feeding improved the effects of high fat diet on villi height and goblet cells, but not liver adiposity. A) Average number of red pixels from oil red O staining images for each group. B) Average villi lengths for each group. C) Average number of goblet cells per crypt for each group. Below: representative images of Alcian Blue stain used to quantify goblet cells. LF=low fat, HF=high fat, HF-PF=high fat-pair-fed. n=4/group. Scale bar = 200 µm. Data presented as mean ± SEM; $^{a, b, c}$ different letters indicate statically significant ($p < 0.05$) differences among groups.

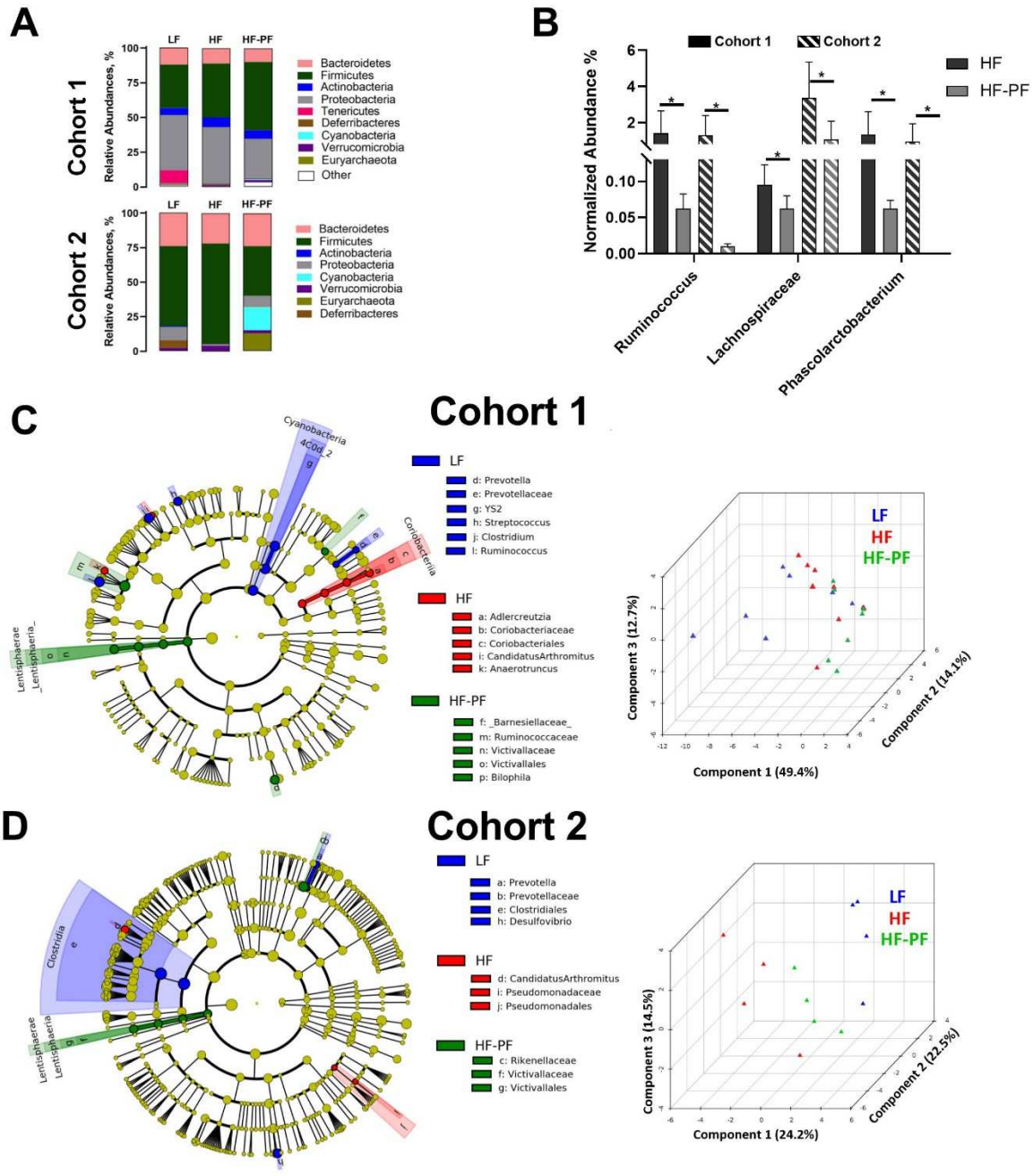

Figure 3.4. Pair-feeding improved microbiota dysbiosis. A) Percent relative abundance of phyla on normalized data (MetagenAssist). B) Statistically significant MetagenAssist normalized abundances consistent between cohorts. C-D) Cladogram run on GALAXY with LDA 1.5 between groups and Partial Least Square Discriminant Analysis (PLS-DA) run on 529 (C) and 458 (D) normalized genus abundances

data points. Cohort 1 n=7-8/group, cohort 2 n=4/group. LF=low fat, HF=high fat, HF-PF=high fat-pair-fed. Data presented as mean ± SEM; * indicate statically significant ($p < 0.05$) differences among groups.

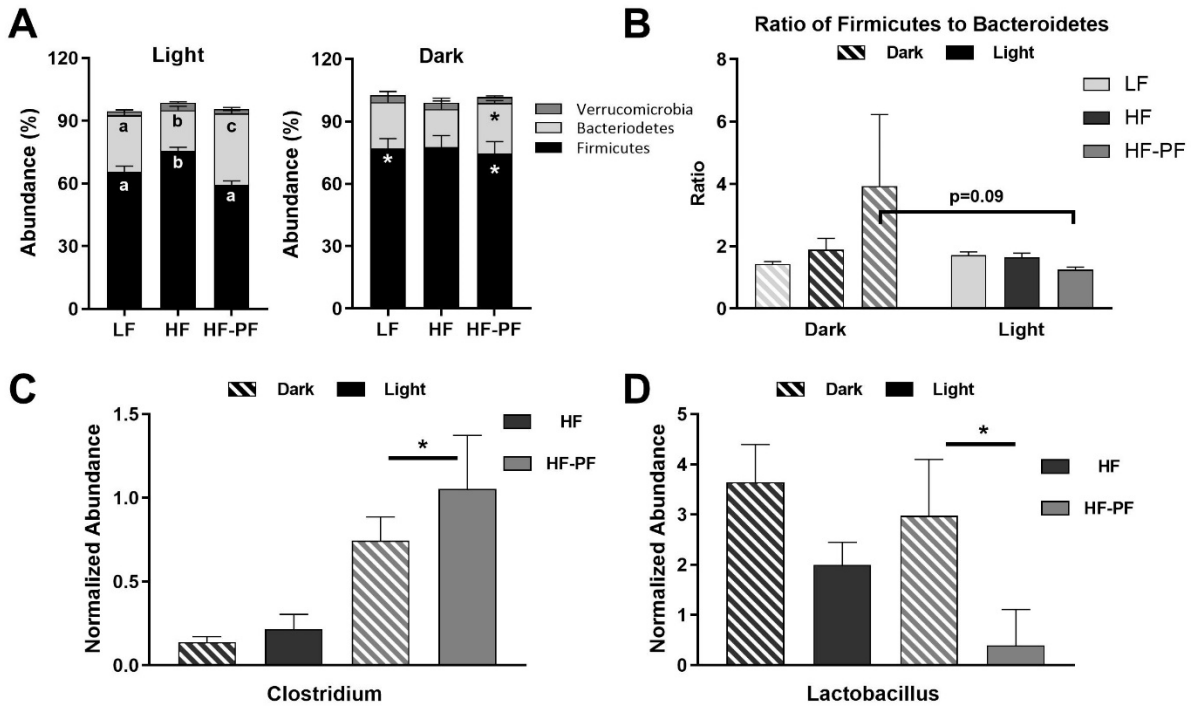

Figure 3.5. Pair-feeding affected microbiota fluctuation between light:dark cycles. A) Abundance percentage fluctuations between light and dark cycles. B) Average *Firmicutes* to *Bacteroidetes* ratios for dark and light cycles during week 5. C-D) Average normalized abundances of *Clostridium* and *Lactobacillus* during dark and light periods. LF=low fat, HF=high fat, HF-PF=high fat-pair-fed. n=4/group. Data presented as mean ± SEM. $^{*;\ a,b,c}$ indicate statically significant ($p < 0.05$) differences among groups.

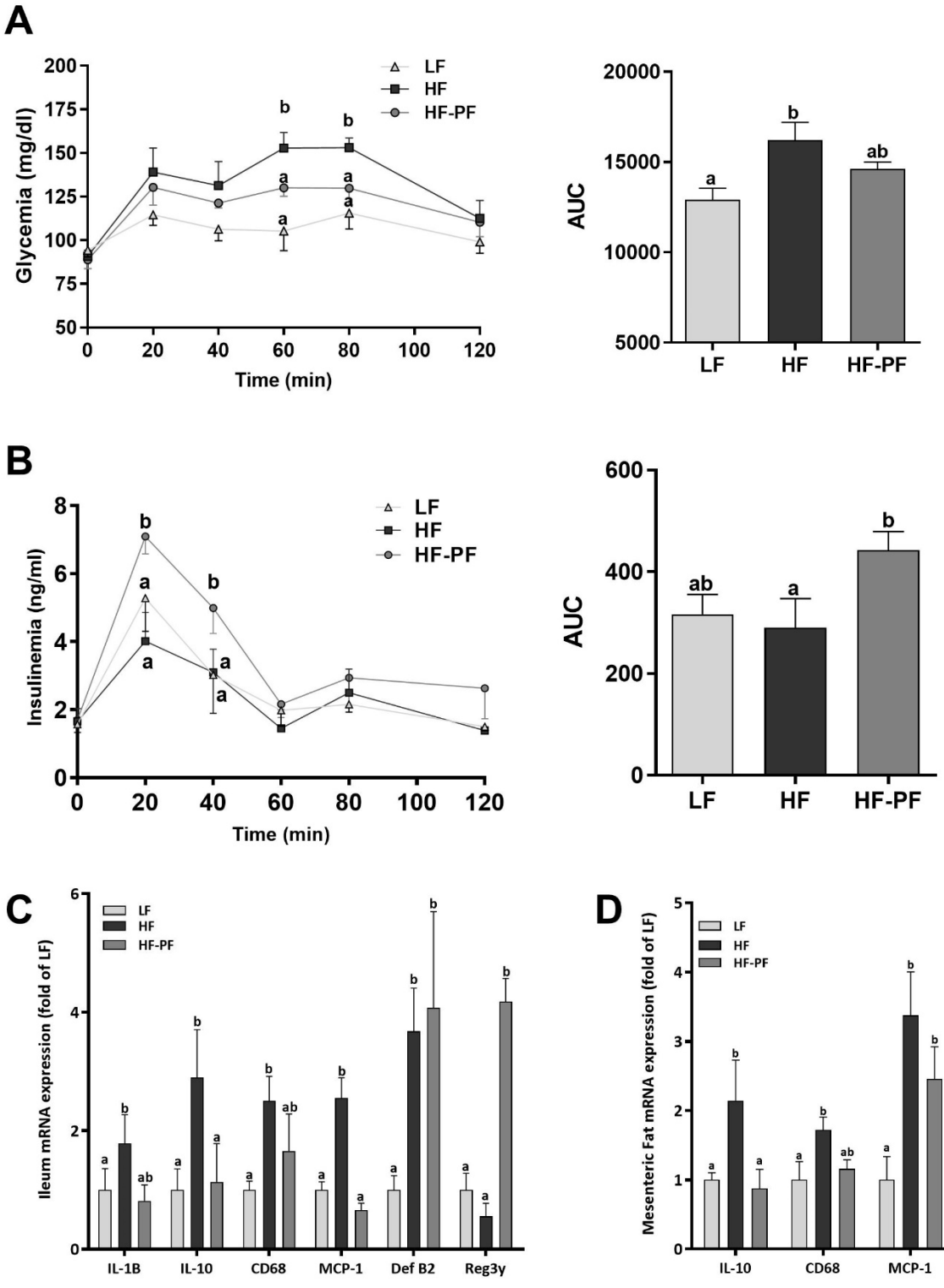

Figure 3.6. Pair-feeding improved inflammation status and glucose tolerance. A) Average blood glucose levels following an oral glucose challenge. B) Average insulin levels from serum collected at regular

intervals following an oral glucose challenge. C) Gene expression of IL-1B, IL-10, CD68, MCP-1, Def B2 and Reg3γ in Ileum. D) Gene expression of IL-10, CD68 and MCP-1 in mesenteric fat. LF=low fat, HF=high fat, HF-PF=high fat-pair-fed, IL-1B=interleukin-1 beta, IL-10=interleukin 10, CD-68=cluster of differentiation 68, MCP-1=Monocyte chemoattractant protein-1, Def B2=beta-defensin 2, Reg3γ=regenerating islet-derived protein 3 gamma. n=4/group. Data presented as mean ± SEM; [a, b, c] different letters indicate statically significant ($p < 0.05$) differences among groups.

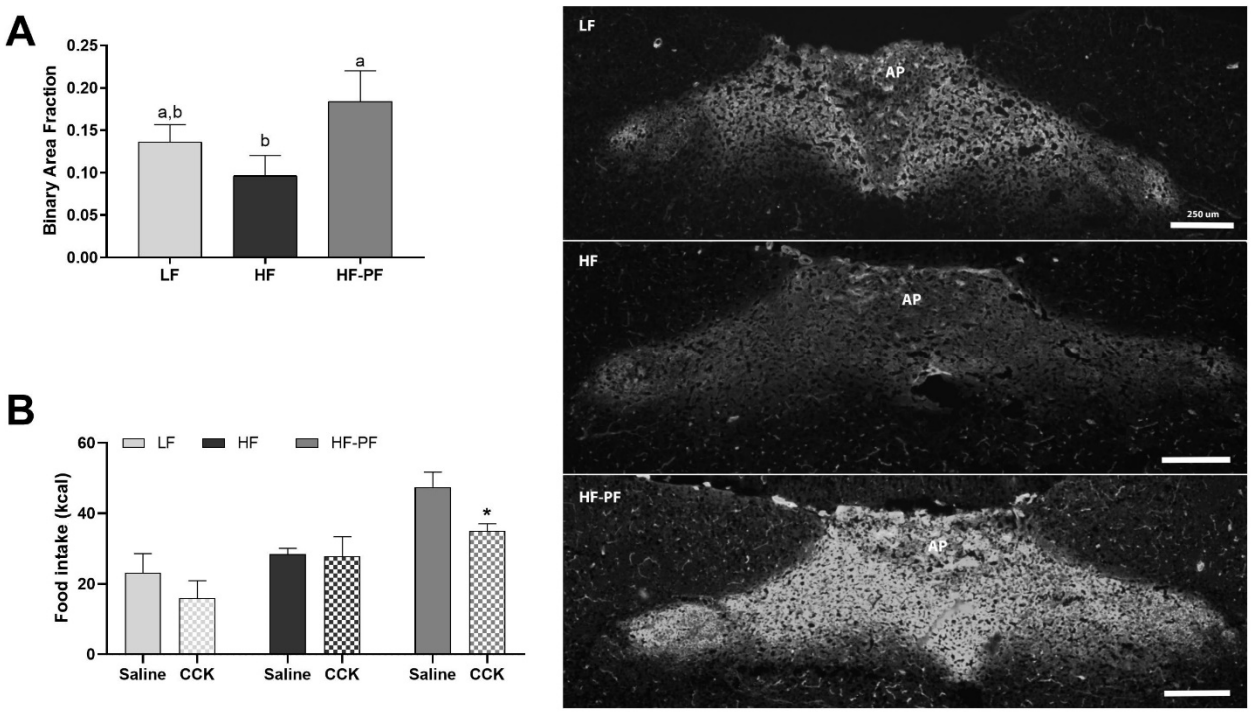

Figure 3.7. Pair-feeding improved vagal remodeling and restored CCK signaling. A) Binary Area Fraction of IB4 staining in the NTS for each diet group. B) Average difference in calories consumed after CCK injection versus injection with a vehicle for each diet group. LF=low fat, HF=high fat, HF-PF=high fat-pair-fed. n=4/group. Data presented as mean ± SEM; [a, b, c] different letters or * indicate statically significant ($p < 0.05$) differences among groups.

CHAPTER 4

CONCLUSIONS

The objective of this dissertation was to investigate the effects of dietary interventions in prevention of the negative metabolic outcomes related to high-fat (HF) diet. I hypothesized that promoting a gut microbiota composition in rodents closer to a control low fat (LF) diet would attenuate the effects of HF diet. Currently, there is little research investigating potential diet interventions to maintain gut microbiota composition, preserve gut integrity and gut-brain signaling. Defined as a chronic state of low-grade inflammation, obesity may be promoted through decreased gut integrity. Microbiota composition has been shown to play a role in the maintenance of gut barrier integrity and modulation of microbiota composition may prevent the development of obesity. The study in Chapter 2 was designed to understand the potential protective effects of potato resistant starch (RS) supplementation on gut microbiota composition, inflammatory status and gut-brain signaling in diet-induced obesity rodents. My hypothesis was that potato RS supplementation would protect the gut microbiota composition and promote production of short-chain fatty acids (SCFAs), preventing low-grade inflammation and preserving gut-brain communication. Potato RS supplementation prevented dysbiosis and increased fecal SCFA content, promoting gut integrity. Functionally, RS supplementation prevented HF diet-induced hyperphagia and maintained glucose homeostasis and vagally-mediated cholecystokinin (CCK) satiety sensitivity. Overall, potato RS supplementation attenuated the effects of HF feeding.

The study in Chapter 3 was designed to investigate the effects of meal patterns on gut microbiota composition and metabolic health. I hypothesized that time restricted feeding patterns

would improve microbiota composition in animals on HF, improving overall metabolic health. Pair-feeding shifted microbiota composition towards that associated with a LF diet and restored circadian fluctuations in microbial abundances. Pair-fed animals also maintained glucose homeostasis likely due to their robust insulin secretion in response to an oral glucose challenge. Functionally, pair-feeding reduced inflammatory status and maintained vagally-mediated CCK-satiation signaling, as shown through maintenance of hindbrain unmyelinated vagal c fibers.

Together, the data presented in Chapters 2 and 3 support a beneficial effect of microbiota manipulation via meal patterning and prebiotic RS supplementation. Both timing of feeding and RS supplementation maintained glucose homeostasis and satiation signaling despite a HF diet composition. Microbiota manipulation via these methods may be a promising treatment for the prevention of obesity and related comorbidities. There are some limitations to the data presented in this dissertation. First, rodent models were used in both studies and thusly the data are not directly translatable to humans. Though, animal research provides the opportunity to develop mechanistic models that may contribute to human treatments. Notably, neither RS supplementation nor pair-feeding completely prevented the effects of HF feeding. Therefore, these treatments alone do not completely reverse the onset of metabolic disorders. Both interventions were prevention paradigms; future research may investigate their potential as treatments for obesity and obesity-related comorbidities. Also, due to difference in adiposity, we cannot confirm that microbiota changes alone drove the metabolic changes and in this case the use of germ-free animals would be an effective model to determine the role of specific microbial strains and gut microbiota compositions. Future investigations should utilize germ-free animals to determine major bacterial players that are driving the metabolic effects related to gut microbiota composition.

REFERENCES

1. Hruby, A. and F.B. Hu, *The Epidemiology of Obesity: A Big Picture.* PharmacoEconomics, 2015. **33**(7): p. 673-689.

2. Monteiro, R. and I. Azevedo, *Chronic inflammation in obesity and the metabolic syndrome.* Mediators of inflammation, 2010. **2010**: p. 289645.

3. de La Serre, C.B., et al., *Propensity to high-fat diet-induced obesity in rats is associated with changes in the gut microbiota and gut inflammation.* Am J Physiol Gastrointest Liver Physiol, 2010. **299**(2): p. G440-448.

4. Klingbeil, E. and C.B. de La Serre, *Microbiota modulation by eating patterns and diet composition: impact on food intake.* American Journal of Physiology-Regulatory, Integrative and Comparative Physiology, 2018. **315**(6): p. R1254-R1260.

5. Lee, S., et al., *Blueberry Supplementation Influences the Gut Microbiota, Inflammation, and Insulin Resistance in High-Fat-Diet–Fed Rats.* The Journal of Nutrition, 2018. **148**(2): p. 209-219.

6. Sen, T., et al., *Diet-driven microbiota dysbiosis is associated with vagal remodeling and obesity.* Physiol Behav, 2017. **173**: p. 305-317.

7. Rajilic-Stojanovic, M., H. Smidt, and W.M. de Vos, *Diversity of the human gastrointestinal tract microbiota revisited.* Environ Microbiol, 2007. **9**(9): p. 2125-36.

8. Ley, R.E., et al., *Microbial ecology: human gut microbes associated with obesity.* Nature, 2006. **444**(7122): p. 1022-3.

9. Ding, S., et al., *High-fat diet: bacteria interactions promote intestinal inflammation which precedes and correlates with obesity and insulin resistance in mouse.* PLoS One, 2010. **5**(8): p. e12191.

10. David, L.A., et al., *Diet rapidly and reproducibly alters the human gut microbiome.* Nature, 2014. **505**(7484): p. 559-563.

11. Cani, P.D., et al., *Metabolic endotoxemia initiates obesity and insulin resistance.* Diabetes, 2007. **56**(7): p. 1761-72.

12. de La Serre, C.B., G. de Lartigue, and H.E. Raybould, *Chronic exposure to low dose bacterial lipopolysaccharide inhibits leptin signaling in vagal afferent neurons.* Physiology & behavior, 2015. **139**: p. 188-194.

13. Vaughn, A.C., et al., *Energy-dense diet triggers changes in gut microbiota, reorganization of gut-brain vagal communication and increases body fat accumulation.* Acta neurobiologiae experimentalis, 2017. **77**(1): p. 18-30.

14. Kant, A.K., *Consumption of energy-dense, nutrient-poor foods by adult Americans: nutritional and health implications. The third National Health and Nutrition Examination Survey, 1988–1994.* The American Journal of Clinical Nutrition, 2000. **72**(4): p. 929-936.

15. Turnbaugh, P.J., et al., *Diet-induced obesity is linked to marked but reversible alterations in the mouse distal gut microbiome.* Cell Host Microbe, 2008. **3**(4): p. 213-23.

16. Cândido, F.G., et al., *Impact of dietary fat on gut microbiota and low-grade systemic inflammation: mechanisms and clinical implications on obesity.* International Journal of Food Sciences and Nutrition, 2017: p. 1-19.

17. Shin, N.R., T.W. Whon, and J.W. Bae, *Proteobacteria: microbial signature of dysbiosis in gut microbiota.* Trends Biotechnol, 2015. **33**(9): p. 496-503.

18. Yu, S. and N. Gao, *Compartmentalizing Intestinal Epithelial Cell Toll-like Receptors for Immune Surveillance.* Cellular and molecular life sciences : CMLS, 2015. **72**(17): p. 3343-3353.

19. Hiippala, K., et al., *Mucosal Prevalence and Interactions with the Epithelium Indicate Commensalism of Sutterella spp.* Frontiers in Microbiology, 2016. **7**: p. 1706.

20. Turner, J.R., *Molecular basis of epithelial barrier regulation: from basic mechanisms to clinical application.* Am J Pathol, 2006. **169**(6): p. 1901-9.

21. Erridge, C., et al., *A high-fat meal induces low-grade endotoxemia: evidence of a novel mechanism of postprandial inflammation.* The American Journal of Clinical Nutrition, 2007. **86**(5): p. 1286-1292.

22. Islam, K.B.M.S., et al., *Bile Acid Is a Host Factor That Regulates the Composition of the Cecal Microbiota in Rats.* Gastroenterology. **141**(5): p. 1773-1781.

23. Wahlstrom, A., et al., *Intestinal Crosstalk between Bile Acids and Microbiota and Its Impact on Host Metabolism.* Cell Metab, 2016. **24**(1): p. 41-50.

24. Cani, P.D., et al., *Selective increases of bifidobacteria in gut microflora improve high-fat-diet-induced diabetes in mice through a mechanism associated with endotoxaemia.* Diabetologia, 2007. **50**(11): p. 2374-2383.

25. Membrez, M., et al., *Gut microbiota modulation with norfloxacin and ampicillin enhances glucose tolerance in mice.* Faseb J, 2008. **22**(7): p. 2416-2426.

26. Rabot, S., et al., *High fat diet drives obesity regardless the composition of gut microbiota in mice.* Sci Rep, 2016. **6**: p. 32484.

27. Magnusson, K.R., et al., *Relationships between diet-related changes in the gut microbiome and cognitive flexibility.* Neuroscience, 2015. **300**: p. 128-40.

28. Noble, E.E., et al., *Early-Life Sugar Consumption Affects the Rat Microbiome Independently of Obesity.* The Journal of Nutrition, 2017. **147**(1): p. 20-28.

29. Stengel, A., et al., *High-protein diet selectively reduces fat mass and improves glucose tolerance in Western-type diet-induced obese rats.* American Journal of Physiology - Regulatory, Integrative and Comparative Physiology, 2013. **305**(6): p. R582-R591.

30. Wang, L., et al., *High-protein diet improves sensitivity to cholecystokinin and shifts the cecal microbiome without altering brain inflammation in diet-induced obesity in rats.* American Journal of Physiology - Regulatory, Integrative and Comparative Physiology, 2017. **313**(4): p. R473-R486.

31. Roopchand, D.E., et al., *Dietary Polyphenols Promote Growth of the Gut Bacterium Akkermansia muciniphila and Attenuate High-Fat Diet–Induced Metabolic Syndrome.* Diabetes, 2015. **64**(8): p. 2847-2858.

32. Belzer, C. and W.M. de Vos, *Microbes inside--from diversity to function: the case of Akkermansia.* ISME J, 2012. **6**(8): p. 1449-58.

33. Mortensen PB, C.M., *Short-chain faty acids in the human colon: relation to gastrointestinal health and disease.* Scand J Gastroenterol Suppl., 1996(216): p. 132-48.

34. Everard A, B.C., Geurts L, Ouwerkerk JP, Druart C, Bindels LB, Guiot Y, Derrien M, Muccioli GG, Delzenne NM, de Vos WM, Cani PD, *Cross-talk between Akkermansia muciniphila and intestinal epithelium controls diet-induced obesity.* Proc Natl Acad Sci USA, 2013. **110**(22): p. 9066-9071.

35. Dao, M.C., et al., *Akkermansia muciniphila and improved metabolic health during a dietary intervention in obesity: relationship with gut microbiome richness and ecology.* Gut, 2016. **65**(3): p. 426-36.

36. Chassaing, B., et al., *Lack of soluble fiber drives diet-induced adiposity in mice.* American Journal of Physiology - Gastrointestinal and Liver Physiology, 2015. **309**(7): p. G528-G541.

37. Cooper, D.N., et al., *The Effects of Moderate Whole Grain Consumption on Fasting Glucose and Lipids, Gastrointestinal Symptoms, and Microbiota.* Nutrients, 2017. **9**(2): p. 173.

38. Roediger, W.E., *Role of anaerobic bacteria in the metabolic welfare of the colonic mucosa in man.* Gut, 1980. **21**(9): p. 793-798.

39. Duncan, S.H., et al., *The role of pH in determining the species composition of the human colonic microbiota.* Environ Microbiol, 2009. **11**(8): p. 2112-22.

40. Tolhurst, G., et al., *Short-chain fatty acids stimulate glucagon-like peptide-1 secretion via the G-protein–coupled receptor FFAR2.* Diabetes, 2012. **61**(2): p. 364-371.

41. Delzenne, N.M., et al., *Impact of inulin and oligofructose on gastrointestinal peptides.* British Journal of Nutrition, 2007. **93**(S1): p. S157-S161.

42. Wu, G.D., et al., *Linking Long-Term Dietary Patterns with Gut Microbial Enterotypes.* Science (New York, N.y.), 2011. **334**(6052): p. 105-108.

43. Zarrinpar, A., et al., *Diet and Feeding Pattern Affect the Diurnal Dynamics of the Gut Microbiome.* Cell metabolism, 2014. **20**(6): p. 1006-1017.

44. Olsen, M.K., et al., *Time-restricted feeding on weekdays restricts weight gain: A study using rat models of high-fat diet-induced obesity.* Physiol Behav, 2017. **173**: p. 298-304.

45. Patterson, R.E. and D.D. Sears, *Metabolic Effects of Intermittent Fasting.* Annual Review of Nutrition, 2017. **37**(1): p. 371-393.

46. Kaczmarek, J.L., S.M. Musaad, and H.D. Holscher, *Time of day and eating behaviors are associated with the composition and function of the human gastrointestinal microbiota.* The American Journal of Clinical Nutrition, 2017.

47. de Lartigue, G., C.B. de La Serre, and H.E. Raybould, *Vagal afferent neurons in high fat diet-induced obesity; intestinal microflora, gut inflammation and cholecystokinin.* Physiol Behav, 2011.

48. Köhler, H., B.A. McCormick, and W.A. Walker, *Bacterial-Enterocyte Crosstalk: Cellular Mechanisms in Health and Disease.* Journal of Pediatric Gastroenterology and Nutrition, 2003. **36**(2): p. 175-185.

49. Amar, J., et al., *Energy intake is associated with endotoxemia in apparently healthy men.* The American Journal of Clinical Nutrition, 2008. **87**(5): p. 1219-1223.

50. Kim, F., et al., *Toll-Like Receptor-4 Mediates Vascular Inflammation and Insulin Resistance in Diet-Induced Obesity.* Circulation Research, 2007. **100**(11): p. 1589-1596.

51. Moran TH, B.A., Salorio CF, Lowery T, Schwartz GJ, *Vagal afferent and efferent contributions to the inhibition of food intake by cholecystokinin.* American Journal of Physiology, 1997. **4 Pt 2**(272): p. R1245-1251.

52. Kentish, S., et al., *Diet-induced adaptation of vagal afferent function.* The Journal of Physiology, 2012. **590**(Pt 1): p. 209-221.

53. Gakis, G., et al., *Neuronal activation in the nucleus of the solitary tract following jejunal lipopolysaccharide in the rat.* Auton Neurosci, 2009. **148**(1-2): p. 63-8.

54. Dudele, A., et al., *Chronic exposure to low doses of lipopolysaccharide and high-fat feeding increases body mass without affecting glucose tolerance in female rats.* Physiological reports, 2015. **3**(11): p. e12584.

55. Foster, S.L. and R. Medzhitov, *Gene-specific control of the TLR-induced inflammatory response.* Clinical immunology (Orlando, Fla.), 2009. **130**(1): p. 7-15.

56. Bjørbæk, C., et al., *Identification of SOCS-3 as a Potential Mediator of Central Leptin Resistance.* Molecular Cell, 1998. **1**(4): p. 619-625.

57. de Lartigue, G., et al., *Leptin Resistance in Vagal Afferent Neurons Inhibits Cholecystokinin Signaling and Satiation in Diet Induced Obese Rats.* PLoS ONE, 2012. **7**(3): p. e32967.

58. Arias-Salvatierra, D., et al., *Role of nitric oxide produced by iNOS through NF-κB pathway in migration of cerebellar granule neurons induced by Lipopolysaccharide.* Cellular Signalling, 2011. **23**(2): p. 425-435.

59. Borner, T., et al., *Lipopolysaccharide inhibits ghrelin-excited neurons of the arcuate nucleus and reduces food intake via central nitric oxide signaling.* Brain, Behavior, and Immunity, 2012. **26**(6): p. 867-879.

60. Riediger, T., et al., *Involvement of nitric oxide in lipopolysaccharide induced anorexia.* Pharmacology Biochemistry and Behavior, 2010. **97**(1): p. 112-120.

61. Kollarik, M., F. Ru, and M. Brozmanova, *Vagal afferent nerves with the properties of nociceptors.* Autonomic neuroscience : basic & clinical, 2010. **153**(1-2): p. 12-20.

62. Ryu, V., Z. Gallaher, and K. Czaja, *Plasticity of nodose ganglion neurons after capsaicin- and vagotomy-induced nerve damage in adult rats.* Neuroscience, 2010. **167**(4): p. 1227-1238.

63. Kettenmann, H., et al., *Physiology of microglia.* Physiol Rev, 2011. **91**(2): p. 461-553.

64. Borsody, M.K. and J.M. Weiss, *The subdiaphragmatic vagus nerves mediate activation of locus coeruleus neurons by peripherally administered microbial substances.* Neuroscience, 2005. **131**(1): p. 235-245.

65. De Vadder, F., et al., *Microbiota-Generated Metabolites Promote Metabolic Benefits via Gut-Brain Neural Circuits.* Cell, 2014. **156**(1): p. 84-96.

66. Erny, D., et al., *Host microbiota constantly control maturation and function of microglia in the CNS.* Nature neuroscience, 2015. **18**(7): p. 965-977.

67. Roth , J., et al., *The Evolutionary Origins of Hormones, Neurotransmitters, and Other Extracellular Chemical Messengers.* New England Journal of Medicine, 1982. **306**(9): p. 523-527.

68. Al-Asmakh, M. and F. Zadjali, *Use of Germ-Free Animal Models in Microbiota-Related Research.* J Microbiol Biotechnol, 2015. **25**(10): p. 1583-8.

69. Chassaing, B., et al., *Dietary emulsifiers impact the mouse gut microbiota promoting colitis and metabolic syndrome.* Nature, 2015. **519**(7541): p. 92-6.

70. Elderman, M., et al., *Sex and strain dependent differences in mucosal immunology and microbiota composition in mice.* Biol Sex Differ, 2018. **9**(1): p. 26.

71. Ng, M., et al., *Global, regional, and national prevalence of overweight and obesity in children and adults during 1980–2013: a systematic analysis for the Global Burden of Disease Study 2013.* The Lancet, 2014. **384**(9945): p. 766-781.

72. Lin, S., et al., *Development of high fat diet-induced obesity and leptin resistance in C57Bl/6J mice.* International Journal Of Obesity, 2000. **24**: p. 639.

73. Johnston, J.D., *Physiological responses to food intake throughout the day.* Nutr Res Rev, 2014. **27**(1): p. 107-18.

74. Kant, A.K. and B.I. Graubard, *40-year trends in meal and snack eating behaviors of American adults.* J Acad Nutr Diet, 2015. **115**(1): p. 50-63.

75. Kohsaka, A., et al., *High-fat diet disrupts behavioral and molecular circadian rhythms in mice.* Cell Metab, 2007. **6**(5): p. 414-21.

76. Qian, J. and F.A.J.L. Scheer, *Circadian System and Glucose Metabolism: Implications for Physiology and Disease.* Trends in endocrinology and metabolism: TEM, 2016. **27**(5): p. 282-293.

77. Zarrinpar, A., et al., *Diet and feeding pattern affect the diurnal dynamics of the gut microbiome.* Cell Metab, 2014. **20**(6): p. 1006-17.

78. Bastard, J.P.*e.a.*, *Recent advances in the relationship between obesity, inflammation, and insulin resistance.* European Cytokine Network, 2006. **17**: p. 4-12.

79. de Lartigue, G., C.B. de La Serre, and H.E. Raybould, *Vagal afferent neurons in high fat diet-induced obesity; intestinal microflora, gut inflammation and cholecystokinin.* Physiol Behav, 2011. **105**(1): p. 100-5.

80. Wu, G.D., et al., *Linking long-term dietary patterns with gut microbial enterotypes.* Science, 2011. **334**(6052): p. 105-8.

81. Chaix, A., et al., *Time-restricted feeding is a preventative and therapeutic intervention against diverse nutritional challenges.* Cell Metab, 2014. **20**(6): p. 991-1005.

82. Caporaso, J.G., et al., *QIIME allows analysis of high-throughput community sequencing data.* Nature methods, 2010. **7**(5): p. 335-336.

83. DeSantis, T.Z., et al., *Greengenes, a chimera-checked 16S rRNA gene database and workbench compatible with ARB.* Applied and environmental microbiology, 2006. **72**(7): p. 5069-5072.

84. Livak, K.J. and T.D. Schmittgen, *Analysis of Relative Gene Expression Data Using Real-Time Quantitative PCR and the 2−ΔΔCT Method.* Methods, 2001. **25**(4): p. 402-408.

85. Hunter, D.A., et al., *Binary imaging analysis for comprehensive quantitative histomorphometry of peripheral nerve.* Journal of Neuroscience Methods, 2007. **166**(1): p. 116-124.

86. Arndt, D.X., Jianguo; Liu, Yifeng; Zhou, You; Guo, An Chi ; Cruz, Joseph A.; Sinelnikov, Igor; Budwill, Karen ; Nesbø, Camilla L.; Wishart, David S., *METAGENassist: A comprehensive web server for comparative metagenomics.* Nucleic Acids Research, 2012. **Jul;40**: p. W88-95.

87. Lee, S., et al., *Beneficial Effects of Non-Encapsulated or Encapsulated Probiotic Supplementation on Microbiota Composition, Intestinal Barrier Functions, Inflammatory Profiles, and Glucose Tolerance in High Fat Fed Rats.* Nutrients, 2019. **11**(9): p. 1975.

88. Martire, S.I., et al., *Altered feeding patterns in rats exposed to a palatable cafeteria diet: increased snacking and its implications for development of obesity.* PloS one, 2013. **8**(4): p. e60407-e60407.

89. Olsen, M.K., et al., *Time-restricted feeding on weekdays restricts weight gain: A study using rat models of high-fat diet-induced obesity.* Physiology & Behavior, 2017. **173**: p. 298-304.

90. Liu, Z., et al., *Gut microbiota mediates intermittent-fasting alleviation of diabetes-induced cognitive impairment.* Nature Communications, 2020. **11**(1): p. 855.

91. Stevenson, N., S. Day, and H. Sitren, *Circadian rhythmicity in rat intestinal villus length and cell number.* International journal of chronobiology, 1979. **6**: p. 1-12.

92. Shaw, D., K. Gohil, and M.D. Basson, *Intestinal mucosal atrophy and adaptation.* World journal of gastroenterology, 2012. **18**(44): p. 6357-6375.

93. Thulesen, J., et al., *Diabetic intestinal growth adaptation and glucagon-like peptide 2 in the rat: effects of dietary fibre.* Gut, 1999. **45**(5): p. 672.

94. Kim, Y.S. and S.B. Ho, *Intestinal goblet cells and mucins in health and disease: recent insights and progress.* Current gastroenterology reports, 2010. **12**(5): p. 319-330.

95. Lecomte, V., et al., *Changes in gut microbiota in rats fed a high fat diet correlate with obesity-associated metabolic parameters.* PloS one, 2015. **10**(5): p. e0126931-e0126931.

96. Yin, J., et al., *Administration of Exogenous Melatonin Improves the Diurnal Rhythms of the Gut Microbiota in Mice Fed a High-Fat Diet.* mSystems, 2020. **5**(3): p. e00002-20.

97. Ley, R.E., et al., *Obesity alters gut microbial ecology.* Proceedings of the National Academy of Sciences of the United States of America, 2005. **102**(31): p. 11070-11075.

98. Naito, E., et al., *Beneficial effect of oral administration of Lactobacillus casei strain Shirota on insulin resistance in diet-induced obesity mice.* J Appl Microbiol, 2011. **110**(3): p. 650-7.

99. Kaczmarek, J.L., S.M.A. Musaad, and H.D. Holscher, *Time of day and eating behaviors are associated with the composition and function of the human gastrointestinal microbiota.* The American Journal of Clinical Nutrition, 2017. **106**(5): p. 1220-1231.

100. König, J., et al., *Human Intestinal Barrier Function in Health and Disease.* Clinical and translational gastroenterology, 2016. **7**(10): p. e196-e196.

101. Zhang, Z. and Z. Liu, *Paneth cells: the hub for sensing and regulating intestinal flora.* Science China Life Sciences, 2016. **59**(5): p. 463-467.

102. Bevins, C.L. and N.H. Salzman, *Paneth cells, antimicrobial peptides and maintenance of intestinal homeostasis.* Nature Reviews Microbiology, 2011. **9**(5): p. 356-368.

103. Weisberg, S.P., et al., *Obesity is associated with macrophage accumulation in adipose tissue.* The Journal of clinical investigation, 2003. **112**(12): p. 1796-1808.

104. Lam, Y.Y., et al., *Role of the Gut in Visceral Fat Inflammation and Metabolic Disorders.* Obesity, 2011. **19**(11): p. 2113-2120.

105. Klingbeil, A.E., et al., *Potato-Resistant Starch Supplementation Improves Microbiota Dysbiosis, Inflammation, and Gut–Brain Signaling in High Fat-Fed Rats.* Nutrients, 2019. **11**(11).

106. Tan, J., et al., *Chapter Three - The Role of Short-Chain Fatty Acids in Health and Disease*, in *Advances in Immunology*, F.W. Alt, Editor. 2014, Academic Press. p. 91-119.

107. Cani, P.D., et al., *Gut microbiota fermentation of prebiotics increases satietogenic and incretin gut peptide production with consequences for appetite sensation and glucose response after a meal.* The American Journal of Clinical Nutrition, 2009. **90**(5): p. 1236-1243.

108. Wilcox, G., *Insulin and insulin resistance.* The Clinical biochemist. Reviews, 2005. **26**(2): p. 19-39.

109. Saad, M.J.A., A. Santos, and P.O. Prada, *Linking Gut Microbiota and Inflammation to Obesity and Insulin Resistance.* Physiology, 2016. **31**(4): p. 283-293.

110. Browning, K.N., S. Verheijden, and G.E. Boeckxstaens, *The Vagus Nerve in Appetite Regulation, Mood, and Intestinal Inflammation.* Gastroenterology, 2017. **152**(4): p. 730-744.